Journal Pre-proof

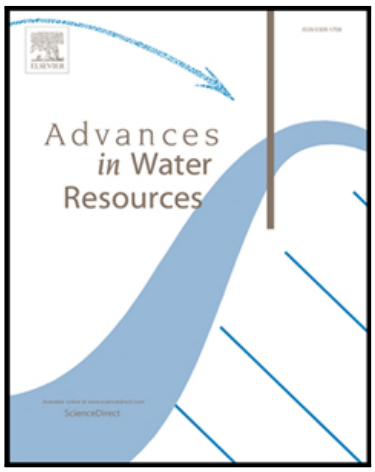

Parameter resolution of simulated responses to periodic hydraulic tomography signals in aquifers

Daniel Paradis , René Lefebvre , Aymen Nefzi

PII: S0309-1708(24)00121-0
DOI: https://doi.org/10.1016/j.advwatres.2024.104734
Reference: ADWR 104734

To appear in: *Advances in Water Resources*

Received date: 5 July 2023
Revised date: 25 March 2024
Accepted date: 25 May 2024

Please cite this article as: Daniel Paradis , René Lefebvre , Aymen Nefzi , Parameter resolution of simulated responses to periodic hydraulic tomography signals in aquifers, *Advances in Water Resources* (2024), doi: https://doi.org/10.1016/j.advwatres.2024.104734

Highlights

- The value of hydraulic tomography with periodic signals is evaluated.
- Transient signals with short periods provide better resolution.
- Resolution is improved by the right combination of periods.
- Optimal periods are linked to hydraulic properties.
- The choice of periods is crucial for optimal results.

ADWR 104734

Parameter resolution of simulated responses to periodic hydraulic tomography signals in aquifers

Daniel Paradis[1], René Lefebvre[2], Aymen Nefzi[2]

[1] Ressources Naturelles Canada - Commission géologique du Canada, 490 rue de la Couronne, Québec, Canada daniel.paradis@nrcan-rncan-.gc.ca

[2] Centre Eau Terre Environnement (INRS-ETE) - Institut national de la recherche scientifique, 490 rue de la Couronne, Québec, Canada

Parameter resolution of simulated responses to periodic hydraulic tomography signals in aquifers

1 Introduction

The estimation of the hydraulic properties of an aquifer is usually based on hydraulic tests in wells. Such tests are carried out by varying the head of a source well and measuring the change in head over time at different points in the aquifer. Various types of hydraulic tests have been developed, with pumping tests and slug tests being common methods [1,2]. In a pumping test, water is pumped from a well, usually at a constant rate, whereas in a slug test, a known volume of water is injected or withdrawn instantaneously. The different methods of head stimulation result in different flow patterns within the aquifer, and analyzing the head associated with each test can therefore provide different information about the hydraulic properties [3,4]. Another method for testing aquifers is to alternately vary the head in the source well (e.g. sinusoidal, square signals). One advantage of periodic testing is that different regions of the aquifer (or support volume) can be investigated simply by varying the signal period, without the need for additional observation wells [e.g. 5,6]. The reason for this is that the penetration depth of the head into the aquifer varies with the period of the signal [e.g. 7].

In early applications, periodic tests were used to estimate the effective hydraulic properties of reservoirs or aquifers. Rasmussen et al [8] conducted sinusoidal aquifer tests in three different aquifers in coastal plain sediments to derive effective transmissivity and storativity values for each aquifer. They tested each aquifer with a single period (1 to 2.5 hours) and found that the results

obtained were generally consistent with conventional pumping tests. However, other field applications using multiple periods found a dependance of the diffusivity (the ratio of transmissivity to storativity) to the period [9,10,11,12,13]. The generally observed relationship is a decrease in effective diffusivity values with increasing period when the pressure responses at the source and observation well are analyzed. Renner and Messar [10] found an opposite relationship when the flow rate and pressure at the source well are used instead. For studies in fractured reservoirs [9,10,11,13], the authors hypothesized that longer periods allow for increased water exchange with smaller fractures, resulting in greater effective storativity and lower hydraulic diffusivity. Cheng and Renner [14], reviewing their previous work [10], pointed out that the variations in diffusivity with periods are due to the "spatial heterogeneity or complexity of the conduits", which are poorly captured by the simple radial flow model used in previous studies to represent flow dynamics during testing. Sayler et al. [15] leveraged this dependence on period to infer the dimensionality of flow or the complexity of fractured aquifers. Fokker et al. [16] also reanalyzed the field observations of [10] using a simple heterogeneous model and showed that heterogeneity can explain the period dependence of diffusivity. An argument used by Cardiff et al. [17], who commented on the results of Becker and Guiltinan [11], and by Rabinovich et al [12] to explain the dependence of effective hydraulic properties on period for periodic tests in a fluvial aquifer.

Because they are indications of the sensitivity of periodic tests to heterogeneity, field work has been conducted with the expectation of improving the representation of heterogeneity by these tests. Lavenue and Marsilly [18] conducted a series of three three-dimensional sinusoidal pumping tests (single period of 72 minutes) in a dolomite aquifer. The calibrated model represented the location of the boundary between the fractured and unfractured regions and was able to reproduce the

amplitudes and phases of a fourth test used as validation data. McElwee et al [19] used a straight ray-based approach to map a fluvial aquifer as a series of "average horizontal" layers between several pairs of wells. The layers were found to generally represent the average of hydraulic conductivity profiles determined by high-resolution slug testing of the well pair. Fokker et al [20] used harmonic injection-recovery tests with 24-hour cycles (single period) to characterize the presence of a conductive fault between two wells in a gas storage field. In doing so, they challenged previous interpretations that had identified an impermeable fault using conventional tests. Fischer et al [21] show that performing tomographic pumping tests with two different periods allows the characterization of different structures within a karst network. They interpreted that the lower period contains information about karstic conduits and the longer period more about the smallest fractures and fissures. Fischer et al [22] also mapped a heterogeneous alluvial aquifer using two source wells with two different periods and recorded the head in 13 observation wells. They found that the "area affected by the pumping can be extended by increasing the period", while the "property maps remain globally similar between the separate inversions and the joint inversion". The resulting maps were coherent with the geology and contamination history of the site. Cardiff et al [23] reported a field application of oscillatory hydraulic tomography with a series of periods (5 to 70 seconds) with an experimental setup that included six isolated source intervals in two wells and 23 observation intervals in three nearby wells in a fluvial aquifer. In a joint inversion with all periods, they found a moderate to strong positive correlation with hydraulic conductivity profiles and volumes obtained by either slug tests or constant pumping rate tomography. As an explanation for these mixed results, reference was made to the different stimulation process in the various methods (e.g. instantaneous slug, constant rate pumping, sinusoidal stimulation).

Even if these field studies provide meaningful results, the fact that the true fields are unknown makes it difficult to derive rules to maximize the benefits of periodic testing. However, few synthetic studies are available. In a numerical study of a simplified petroleum reservoir with concentric heterogeneities around a production well, Rosa and Horne [24] have shown that the choice of periods and location of the observation well can be optimized to obtain the best results in terms of parameter estimation. They have also shown that periodic tests are superior to constant rate pumping tests in resolving heterogeneities, as "changing flow rates yields an increase in the sensitivity of the pressure data to the reservoir properties". In a similar numerical study, Ahn and Horne [25] have shown "that the signals from different frequencies can be used to reveal permeabilities by reflecting different radii of influence from the active well". It was found that for periods with radii of influence within the region between the source well and the observation well, the resolution of heterogeneity increases with the number of periods used. Conversely, the use of periods with radii that extend beyond the observation well does not lead to a correct estimate. Similarly, for a synthetic channel-type aquifer, Cardiff et al [26] have shown that a "progressive improvement in aquifer imaging results can be obtained by then jointly inverting multiple frequencies' responses". This was attributed to the "different spatially distributed sensitivities to aquifer parameters" caused by the different stimulation periods. In contrast to previous studies, Wang et al [27] found in a stochastic analysis of oscillatory hydraulic tomography that "the estimates [of hydraulic properties] from different frequencies and multifrequency tests are indistinguishable on average". They claimed that "the sensitivity maps of the different frequencies are highly correlated", which limits the resolution.

While previous field applications and theoretical developments have shown the benefits of periodic testing, there are still concepts and issues that need to be clarified. The aim of this study is therefore

to further evaluate the information that can be obtained from periodic tests carried out in wells, focusing on the spatial resolution of hydraulic properties. Methods that use natural tidal fluctuations to estimate the hydraulic properties of aquifers [7,28,29,30,31,32,33] have similarities to periodic tests performed in wells. Although tidal influences can be detected at considerable distances from the shoreline, the signal typically results from a complex superposition of different processes that are difficult to distinguish in complex hydrogeological contexts [8]. This article therefore focuses on periodic tests in wells, which provide a controlled amplitude and period of the hydraulic perturbation and allow a more comprehensive understanding of the periodicity of the signal. This study refers to hydraulic tests performed in a tomographic configuration selected for its suitability to map the heterogeneity of hydraulic properties. A comprehensive analysis is performed, considering the horizontal hydraulic conductivity (K_h), the vertical anisotropy of hydraulic conductivity (Kv/K_h) and the specific storage (S_s) of aquifers. The tomography experiment involves performing a series of periodic tests at discrete intervals within a source well. The resulting signal is measured within both the source interval and adjacent observation wells also equipped with packers to isolate discrete intervals. Throughout the experiment, the equipment can be repositioned in the wells, enabling the dense recording of head data in various orientations within the plane between the source well and the observation well. Such a of tomographic configuration provides for a better vertical resolution of the aquifer than a tidal source signal covering the entire aquifer thickness.

The study is carried out through a series of numerical groundwater flow simulations combined with a parameter resolution analysis (Section 2). The analysis is performed in the time domain, considering the whole signal with the transient and steady-periodic phases. An analysis of the

results provides information on the expected performance of periodic hydraulic tomography (Section 3). Practical insights for the application and analysis of periodic tests are also discussed.

2 Methods

A numerical groundwater flow model is used to gain insights into the principles of periodic hydraulic testing in a tomographic configuration. For a series of periodic tests, this model generates the heads and sensitivities on which the resolution analysis is based. A resolution matrix expresses the degree of parameter resolution that can be achieved given the physics and geometry of a particular hydraulic experiment [34]. Thus, resolution is a tool that can be used to compare the information content of hydraulic tests carried out with different experimental designs.

2.1 Groundwater flow numerical model

The tomographic periodic tests are simulated with the radial groundwater flow model lr2dinv [35]. This model has been used in several peer-reviewed publications to simulate hydraulic tests in wells [3,36,37,38,39,40,41,42,43,44,45,46]. The hydraulic head h (m) generated in an aquifer by a hydraulic test in a well is described by the radial groundwater flow equation:

$$\frac{1}{r}\frac{\partial}{\partial r}\left(rK_r\frac{\partial h}{\partial r}\right)+\frac{\partial}{\partial z}\left(K_z\frac{\partial h}{\partial z}\right)=S_s\frac{\partial h}{\partial t} \quad (1)$$

where r (m) is the radial coordinate from the center of the well, z (m) is the vertical coordinate, t (s) is the time, S_s (m^{-1}) is the specific storage, and K_r (or K_h) and K_z (ms^{-1}) are the hydraulic conductivities in the radial (or horizontal) and vertical directions, respectively. Equation 1 is solved using a block-centered finite-difference formulation after a logarithmic transformation of the radial

flow equation into an equivalent equation in Cartesian coordinates [4,35]. The simulation results of lr2dinv were compared with the analytical solution of Dougherty and Babu [47] for the same experimental setup to ensure their validity (see Supplementary Material 1).

Two wells with a diameter of 0.0762 m and separated by 8 m are considered (Figure 1). The tomographic configuration consists of seven periodic tests performed sequentially at seven source intervals isolated with packers in the source well (S1 to S7 in Figure 1). For each test, heads are monitored at four locations: the source interval itself and three intervals in the observation well (e.g., O1, O2, and O3 for test S1 in Figure 1). This test configuration is based on previous studies at a test site in order to offer a basis of comparison with actual tomographic field tests [3,44].

The length of each source interval is 0.60 m. Simulation of the effects of wellbore storage and packer placement in the source well is achieved by using the inner boundary of the model to represent the region within the wellbore. A Darcy's Law formulation is used to approximate the processes, with the screened interval represented as a region of high permeability and the packers as impermeable.

A periodic flow rate Q (m^3s^{-1}) is imposed in the screened interval to induce water exchange with the aquifer at the screen of the well having a radius r_w (m):

$$Q = \pi r_c^2 \frac{\partial(A_0 \sin(2\pi/T_0 t))}{\partial t} = 2\pi r_w L K_h \frac{\partial h}{\partial r} \quad (2)$$

where r_c (m) is the radius of the casing or riser, L (m) is the length of the source interval, and $A_0 sin(2\pi/T_0\ t)$ (m) is the sinusoidal hydraulic stress, where A_0 (m) and T_0 (s) are the peak amplitude and period of the periodic stress, respectively. In the field, periodic flow can be achieved 1) mechanically with a movable rod controlled by a winch [11,13] or a motorized piston [23], 2) pneumatically by controlling the air pressure above the water level in a pressurized well [15], and 3) hydraulically with a dual-pump system that controls injection and pumping rates [8,10]. For the simulations, the periodic flow rate is approximated as a series of steps, with each step modeled as a constant flow boundary condition with a start and end time.

A simulation grid with an exponential increase in horizontal cell size from the source is used. The horizontal cell size varies from 0.0075 m at the source well to 15.3 m at the outer boundary. A constant spacing of 0.30 m is used for the vertical cell size. The simulation grid is overlaid with a parameter grid (Figure 1). The parameter grid covers the extent of the aquifer, and its cells coincide with the radial and vertical positions of the source and observation intervals. The cells of the first ten columns of the parameter grid between the source and observation wells have a constant width of 1.45 m. Beyond the observation well, starting at a radial distance of 14.55 m, a 74 m wide large parameter grid column represents the hydraulic parameters outside and far from the "focus area" in which hydraulic signals are generated at the source well and measured at the observation well. The same discretization of the parameter grid is used for K_h, K_v/K_h and S_s. The model represents a homogeneous and anisotropic aquifer wedge with the properties summarized in Table 1. The values of the hydraulic properties of a base case are used for simulations 1, 2, and 4, while lower and higher values than those of the base case are used for simulations 3.

Table 1. Hydraulic properties used in simulations.

Simulations	Horizontal hydraulic conductivity, K_h (ms^{-1})	Vertical to horizontal hydraulic conductivity, K_v/K_h (-)	Specific storage, S_s (m^{-1})
Base Case: 1, 2, 4 & 5	$1x10^{-5}$	0.1	$1x10^{-5}$
Lower/Higher: 3	$6x10^{-6}/4x10^{-5}$	0.06/0.4	$6x10^{-6}/4x10^{-5}$

The outer boundary condition at 92 m from the source well is a fixed head and confined flow is specified with zero-flux conditions at the upper and lower boundaries (Figure 1). Static conditions before each hydraulic test simulation are represented with a constant head for the model domain. The "focus area" between the source and observation wells represents the domain in which the hydraulic parameters of the aquifer are better resolved by the head measurements made at the source and observation intervals during the tomographic experiments. This focus area contains 42 parameter grid cells. Through trial and error, the number of cells in the parameter grid was determined to ensure that the distinctive characteristics of the L-curve, as illustrated in Figure 2, were revealed for each period tested.

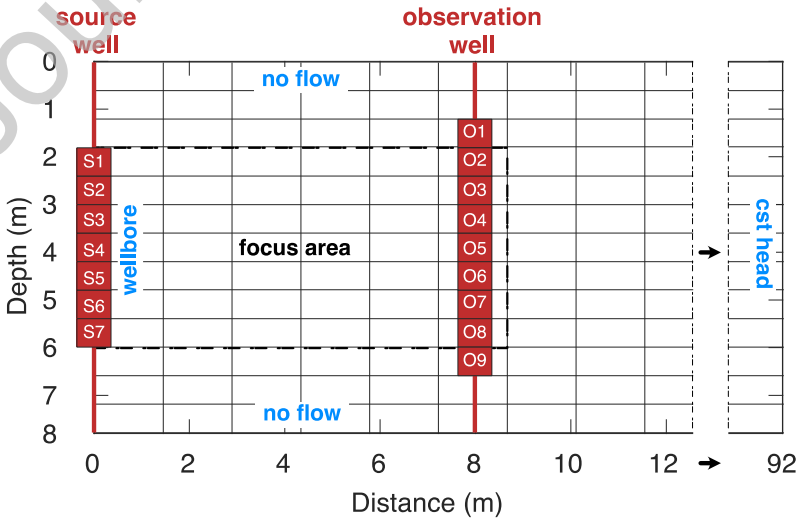

Figure 1. Parameter grid, boundary conditions, and locations of source and observation intervals. The cells within the focus area (dotted black rectangle) are used to calculate the resolution statistics. The parameter grid is superposed on the model numerical grid (not shown).

2.2 Resolution analysis

Following a hydraulic test inducing changes in hydraulic heads in an aquifer, the ability to resolve different hydraulic parameters of the aquifer depends on the relative magnitude and correlation between the sensitivities of the heads to those hydraulic parameters [39,44,48]. Sensitivity expresses the response of the head to a change in the value of a hydraulic parameter. To be resolved, a parameter must have a nontrivial sensitivity value. The greater the difference in the magnitude of the sensitivity of a parameter relative to its surrounding parameters, the better will be its resolution. Moreover, a parameter is better resolved if its sensitivity pattern differs from that of other parameters over time as heads vary following an imposed hydraulic stress.

Although the inverse problem of groundwater flow is nonlinear, the resolution analysis presented in this paper and summarized below is based on a linear approximation of the model behavior in the vicinity of the assumed hydraulic parameters. That is, the sensitivity matrix serves as an approximate linear representation of the nonlinear flow. It is also expected that a resolution analysis based on a radial 2D model is a valid approximation that can be generalized to planar 2D or 3D models. In Supplementary Material 2, it is shown that the resolution for wells in a planar 2D confined aquifer is mainly centered in the plane enclosing the wells with similar patterns to those obtained with a radial model. Nevertheless, the use of a radial model must be carefully considered when dealing with an aquifer characterized by significant heterogeneities that may cause significant

lateral flow outside the plane of the wells. The resolution analysis presented in this paper is performed using the MATLAB (MathWorks, 2023) Regularization Toolbox [49].

2.2.1 Inverse problem

The resolution analysis is based on the study of the inverse problem associated with a specific tomographic experiment. An inverse hydraulic problem involves finding a model for the spatial distribution of the hydraulic parameters of an aquifer for which head data have been measured in wells at different times and locations following an imposed hydraulic stress [34]:

$$\mathbf{m} = F^{-1}(\mathbf{d}) \quad (3)$$

where **m** is a vector of *n* hydraulic parameters that we try to estimate from the head data vector **d** with *m* observations. F^{-1} is the inverse process of the forward operator *F*, which represents the non-linear behavior of groundwater flow, as described in section 2.1. However, the process of finding an inverse solution is challenging and involves important issues such as the existence of the solution (e.g., no model that fits the observations), the uniqueness of the solution (e.g., rank deficiency where many models equally fit the observations) and the instability of the solution process (e.g., ill-conditioning where small changes in the observations lead to very different models) [34].

2.2.2 Generalized inverse

To facilitate the search for an inverse solution **m**, the generalized inverse $\mathbf{J}^{\dagger}$ of the sensitivity matrix **J** is used as the inverse operator F^{-1} [50,51]:

$$\mathbf{m}_{\dagger} = \mathbf{J}^{\dagger}\mathbf{d} \qquad (4)$$

The sensitivity matrix **J** is an *m*-by-*n* normalized sensitivity matrix of *m* observations and *n* parameters, expressing the head response at each observation point and at each time to a change in each hydraulic parameter value:

$$J_{m,n} = \frac{\partial d_m}{\partial m_n / m_n} \qquad (5)$$

This normalized form of the sensitivities is used to better identify the relative influence of each hydraulic parameter [35]. The elements of the sensitivity matrix were evaluated using the sequential perturbation approach of a groundwater flow model developed with the lr2dinv numerical simulator.

The generalized inverse $\mathbf{J}^{\dagger}$ is a decomposition of the sensitivity matrix **J** into its singular values (SVD):

$$\mathbf{J}^{\dagger} = \mathbf{V}\mathbf{S}^{-1}\mathbf{U}^{T}\mathbf{d} \qquad (6)$$

where **U** and **V** form two sets of orthonormal matrices of size *m*-by-*m* and *n*-by-*n*, respectively, and **S** is an *m*-by-*n* diagonal matrix consisting of the singular values s_i of **J** arranged in decreasing size. The generalized inverse always produces the least squares inverse solution with minimum length and ensures that an inverse solution always exists for ill-conditioned and rank deficient hydraulic inverse problems.

2.2.3 Tikhonov regularization

The presence of very small singular values in **S** of Equation (6) can however cause the generalized inverse solution to become extremely unstable [34]. Therefore, regularization of the solution is necessary. One of the most widely used regularization methods is the Tikhonov technique [52]:

$$\mathbf{m}_\lambda = \mathbf{VFS}^\dagger\mathbf{U}^T\mathbf{d} \qquad (7)$$

where an *n*-by-*n* diagonal matrix **F** with diagonal elements given by the filter factors:

$$f_i = \frac{s_i^2}{s_i^2+\lambda^2} \qquad (8)$$

is introduced to reduce the influence of smaller singular values s_i.The weighting of the singular values is determined by λ. If the value of λ is much higher compared to s_i, the value of f_i approaches zero, which leads to a lower weighting. Conversely, a much lower value of λ leads to a higher weighting. The choice of λ is explained in section 2.2.5. The matrix $\mathbf{S}^\dagger$ is the generalized inverse of **S**, $\mathbf{S}^\dagger = \mathbf{V}\boldsymbol{\Sigma}^\dagger\mathbf{U}^T$, in which $\boldsymbol{\Sigma}^\dagger$ is a diagonal matrix where each non-zero diagonal element is the reciprocal of the corresponding non-zero singular value of the original matrix **S**. The zeros on the diagonal of $\mathbf{S}^\dagger$ correspond to the zero singular values of **S**.

2.2.4 Resolution matrix

The concept of resolution is a means of evaluating the properties of the generalized inverse solution of a specific hydraulic experiment. A resolution matrix reflects the physics and geometry of the

experiment. In the Tikhonov regularization method, the resolution matrix of the hydraulic parameter is given by:

$$\mathbf{R}_{m,\lambda} = \mathbf{VFV}^T \quad (9)$$

where the elements of $\mathbf{R}_{m,\lambda}$ indicate the relative magnitude and correlation between the sensitivities of the heads to the hydraulic parameters. Thus, if $\mathbf{R}_{m,\lambda} = \mathbf{I}$, the identity matrix, the resolution is perfect, and the true hydraulic parameters are recovered exactly. At the opposite extreme, a resolution value approaching zero means that a parameter cannot be resolved on the basis of the measured heads.

2.2.5 Selecting an optimal solution

Note that model resolution matrix depends on the value of λ. For consistency among the comparison of the different simulations, we select the λ value according to the L-curve criterion [53]. An L-curve is constructed from the minimization of the damped least squares equation for a range of λ values:

$$min \ \|\mathbf{Jm}_{\boldsymbol{\lambda}} - \mathbf{d}\|_2^2 + \boldsymbol{\lambda}^2 \|\mathbf{m}_{\boldsymbol{\lambda}}\|_2^2 \quad (10)$$

where the left side is the squared norm of the residual of the head data and the right side is the squared norm of the model parameter vector.

Plotted on a logarithmic scale, the curve of the optimal values of the residual and model norms often takes the form of a L (Figure 2). For the horizontal segment of the curve, the solution is

dominated by the regularization error. Very large λ values lead to an over-smoothing of the solutions with a large residual norm. On the other hand, the vertical segment is characterized by very small λ values, which results in over-fitting of the head data. Thus, the optimal solution between sensitivity to noise and parameter resolution is for the value of λ that lies at the corner of the L-curve. The adaptative pruning algorithm by [54] was used to locate the corner of the L-curve for each set of simulations and for all periods described in Table 2.

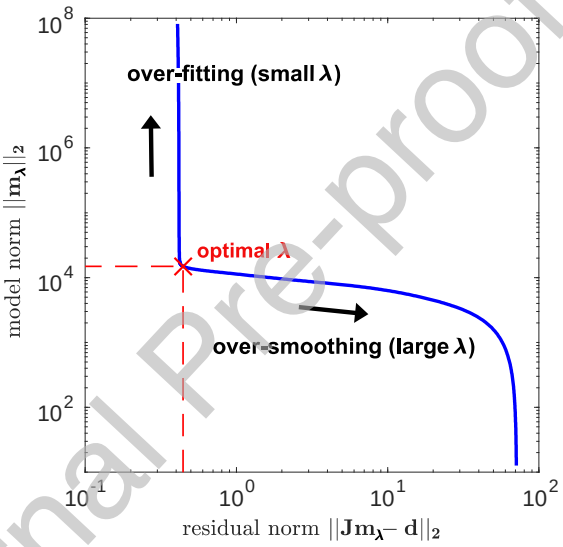

Figure 2. An example of L-curve for the tomographic experiment with tests with a period of 0.5 min in Figure 3. The optimal λ value at the corner of the L-curve is a balance between over-fitting the head data and over-smoothing the estimated hydraulic parameters.

2.2.6 Noise level

To obtain a realistic evaluation of the resolutions, the heads generated by the groundwater flow model must be perturbed by a noise level consistent with field measurements. The noise level is based on a field application of periodic slug tests carried out by the authors. This noise is estimated as normally distributed with an expected 0 mean and a standard deviation of 8.5×10^{-3} and 1.8×10^{-4}

m for the source and observation intervals, respectively. A higher noise is applied to the heads of the source intervals to account for the turbulent flow created by the motion of the rod used to generate the periodic signal.

2.2.7 Metrics

Two different metrics are used to compare the resolution associated to each simulation [55]. First, the total information content (*IC*) of the experiment is assessed by summing all diagonal elements of the model resolution matrix:

$$IC = \sum_i^N R^N_{m,\lambda,ii} \qquad (10)$$

where N is the total number of parameters within the focus area (Figure 1). The higher *IC* is, the better the resolution of the parameter obtained for a given hydraulic experiment.

Then, for each hydraulic property (K_h, K_v/K_h and S_s), the information content IC_j associated with each property (j) is divided by the corresponding number of parameters N_j to obtain the resolution degree (*RD*):

$$RD_j = {IC_j}\Big/{N_j} \qquad (11)$$

where j=1 to 3 and corresponds to K_h, K_v/K_h and S_s, respectively. *RD* is a measure of the average resolution achieved for each hydraulic property, varying between 0 (not resolved) and 1 (perfectly resolved).

2.3 Groundwater flow simulation program

Table 2 summarizes the simulation program whose purpose is to fully explore the effect of test conditions on the hydraulic response, information content and resolution of individual and combined periodic signals. Five sets of simulations are carried out that involve a series of experiments using twelve (12) different periodic signals. Seven tests are simulated for each experiment, and the heads simulated for the 7 source intervals and 21 observation intervals are used for analysis. The twelve (12) periods range from 0.5 to 1024 min for the base scenario in a logarithmic increment to base 2. The choice of periods is based on the time required for a pump test to reach equilibrium or a slug test to return to initial conditions (a reference time of 128 min for the base case). Therefore, periods below and above this reference time are chosen.

The first set of twelve tomographic experiments is simulated for the base case aquifer properties (Table 1), varying the period, and keeping the peak amplitude A_0 of the periodic signal the same for all periods (fixed A_0 test strategy). This set of simulations provides reference conditions that are used to compare the effects of the different test conditions considered in the other simulations (Section 3.1 and Section 3.2). The second set of simulations considers the effects of adjusting A_0 as a function of periods, using larger values of A_0 for longer periods to maintain the same variation in head in the source interval for all periods (explained in Section 3.3). The results obtained with this adjusted A_0 strategy are further analyzed to gain insight into the importance of the transient phase for the resolution of the parameter (Section 3.4). The effect of combining multiple periods is also analyzed using the two test strategies in Section 3.5. The third set of simulations explores the influence of hydraulic parameters on the head and resolution for the test strategy with a fixed A_0 (Section 3.6). Finally, the fourth and fifth set of simulations investigates how the magnitude of

the peak amplitude (A_0) and the ratio of the casing and well radii (r_c/r_w) affect the heads and the resolutions, respectively (Section 3.7).

Table 2. Simulation program (Table 1 provides the values of hydraulic parameters).

Simulations	Hydraulic parameters	Source signal amplitude $2*A_0$ (m)	Periods (min)	Ratio of casing and well radii (r_c/r_w)
1	Base Case	Fixed (4 m)	0.5 to 1024	1
2	Base Case	Adjusted (4 to 84 m)	0.5 to 1024	1
3	Lower/Higher	Fixed (4 m)	Lower K_h: 2 to 4096 Higher K_h: 0.125 to 256	1
4	Base Case	Fixed (2, 4 and 6 m)	0.5 to 1024	1
5	Base Case	Fixed (4 m)	0.5 to 1024	0.71, 1 and 1.41

3 Results and discussion

3.1 Head variation with periods

A first set of twelve tomographic experiments is simulated for the base case aquifer (Simulations 1 in Tables 1 and 2), varying the period, and keeping A_0 the same for all periods (fixed A_0 test strategy). Figure 3 shows that although A_0 is constant for all periods, the resulting head variation in the source interval decreases with increasing periods (slower movement in the source well).

Moreover, the maximum head variation in the observation interval is reached for the 32-min period. Interestingly, this peak is not reached when the head variation in the source interval is maximal.

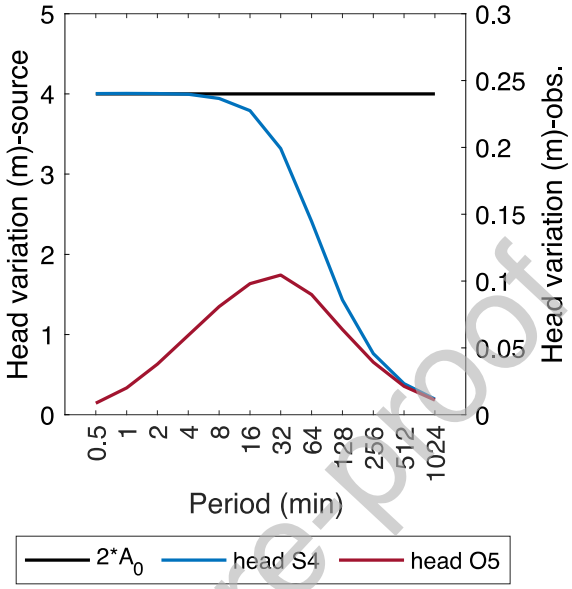

Figure 3. Example of simulated variation of head in a source (S4) and an observation (O5) interval for the base case with fixed peak amplitude A_0 of the periodic signal for twelve selected periods (Simulations 1 in Tables 1 and 2). Head variation is the difference between maximum and minimum head over a cycle when steady state is reached (note the scale difference for the source and observation intervals). The positions of S4 and O5 are shown in Figure 1.

To explain the bell-shaped curve for O5 in Figure 3, the heads at different points between S4 and O5 are extracted from the numerical simulations (Figure 4). Two important observations can be made from Figure 4. First, the head variation in S4 decreases with increasing period (Figure 4a). Looking at the water balance in the source interval for each period (Figure 5a), for the same volume of water injected or pumped (total), the distribution between water flowing through the aquifer (aquifer) and water stored in the well (well) changes with period. That is, the longer the period, or

the slower the water is injected, the more water is exchanged with the aquifer and the lower is the head in the source well (Figure 5b-d).

Also, the attenuation of the head in the aquifer decreases with increasing period (Figure 4a). The attenuation is represented by the slope of the variation of the head with distance from the source well. Attenuation is related to the volume of water flowing through the aquifer (Figure 5a). The larger is this volume, the lower is the attenuation. This is consistent with Jacob's analytical solution [56] generally used to estimate the diffusivity of an aquifer influenced by tides.

In summary, given the different combination of head in the source interval and attenuation, head variations in the observation interval O5 are smaller both for the shorter periods (higher head in the source well but more attenuation) and longer periods (lower head in the source well and lower attenuation in the aquifer). Maximum head variation in the observation interval O5 occurs for the intermediate 32-min period due to the combination of a still relatively high head in the source well and a low attenuation in the aquifer (Figure 3 and Figure 4b). The maximum support volume is then reached with the 32-min period in which the head can reach a greater distance from the source well. Figure 6 also shows that the sensitivities for K_h and K_v/K_h also reach a maximum for this period within the focus area and beyond the observation well. The sensitivity for S_s, however, decreases steadily with increasing period. This suggests that a different support volume can be defined for each hydraulic property based on the sensitivity. This could provide an alternative angle for analyzing periodic tests aimed at estimating the diffusivity value that combines transmissivity and storativity in a single term [e.g. 8,9,10,11,12,13].

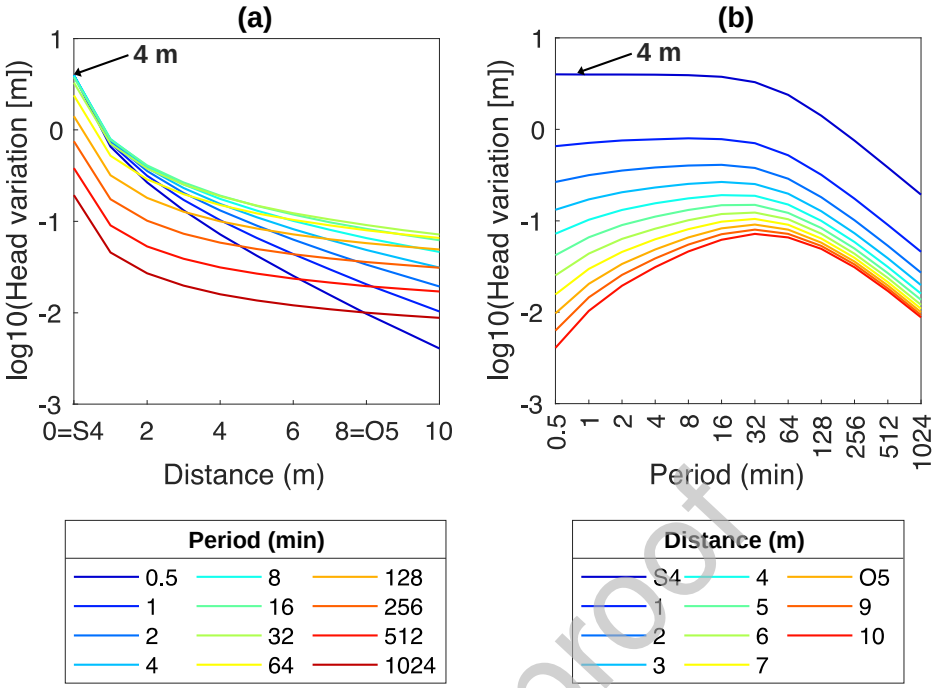

Figure 4. Variation of head with (a) distance from source interval for different periods, and (b) period for different distances. Periodic tests with a fixed peak amplitude A_0 for all periods. The locations of the source (S4) and observation (O5) intervals are shown in Figure 1.

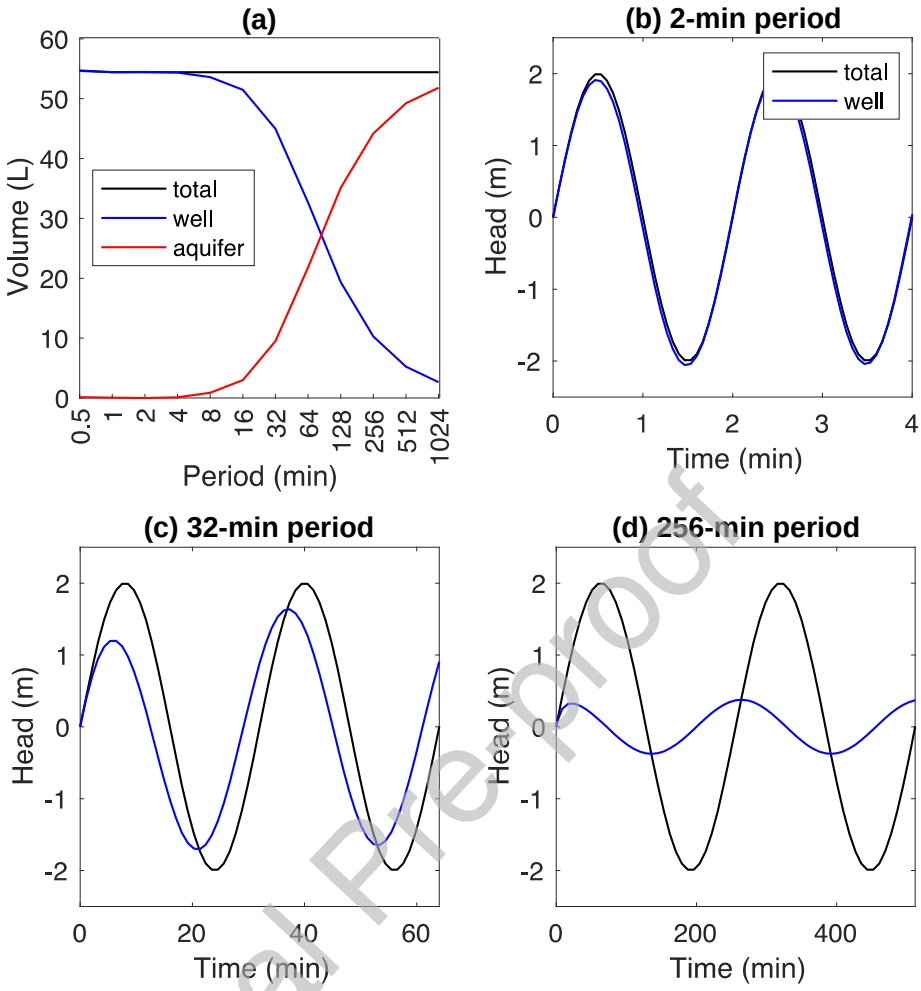

Figure 5. (a) For different periods, variation in volumes (per half cycle) of water injected or pumped into the source interval S4 (total), water flowing through the aquifer (aquifer), and water stored in the well (well). The aquifer volume is the difference between the total and well volumes. Variation of total and simulated (well) heads in source interval S4 for periods: (b) 2 min; (c) 32 min; and (d) 256 min. The total head is a reference point that represents the conversion of the total volume. It indicates the maximum head that can be achieved in the source interval based on the total injected or pumped volume.

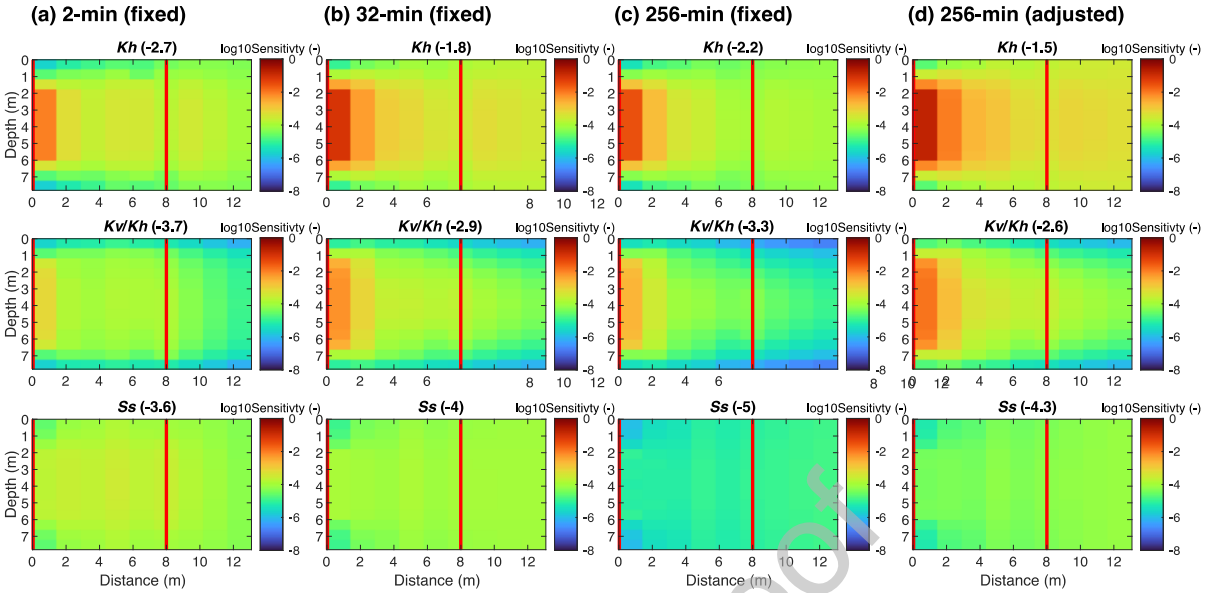

Figure 6. Spatial distribution of RMS (root-mean-square) normalized sensitivities for K_h, K_v/K_h and S_s with the test strategy with fixed A_0 source signal amplitude for three selected periods: (a) 2 min; (b) 32 min; (c) 256 min, and (d) 256-min with the test strategy with variable A_0. The sensitivities are evaluated for the head in the source and observation intervals. The number in the parenthesis next to the name of the hydraulic property is the average RMS sensitivity within the focus area.

3.2 Parameter resolution with periods

Figure 7a shows the analysis of the diagonal elements of the resolution matrix for each of the twelve tomographic experiments of the first series of simulations (Simulations 1 in Tables 1 and 2; Section 3.1). Even though the head is highest in the observation intervals for the 32-min period (Figure 3), the maximum information content and resolution degree are related to the shorter periods (0.5 and 1 min). The resolution degree for all hydraulic properties decreases steadily with period. The decrease is more pronounced for S_s because the variations of head with time decrease with period more than the horizontal and vertical spatial gradients that allow estimation of K_h and K_v/K_h,

respectively. The resolution of K_v/K_h is possible here due to the small aspect ratio (ratio of screen length to screen radius) of the source interval, which results in a larger proportion of vertical flow [43]. Figure 7b shows the resolution for additional simulations with shorter periods than those of the base case. Figure 7b shows that a further reduction of the period does not necessarily lead to an improved resolution because while the head decreases in the observation intervals within the noise level, the resolution deteriorates.

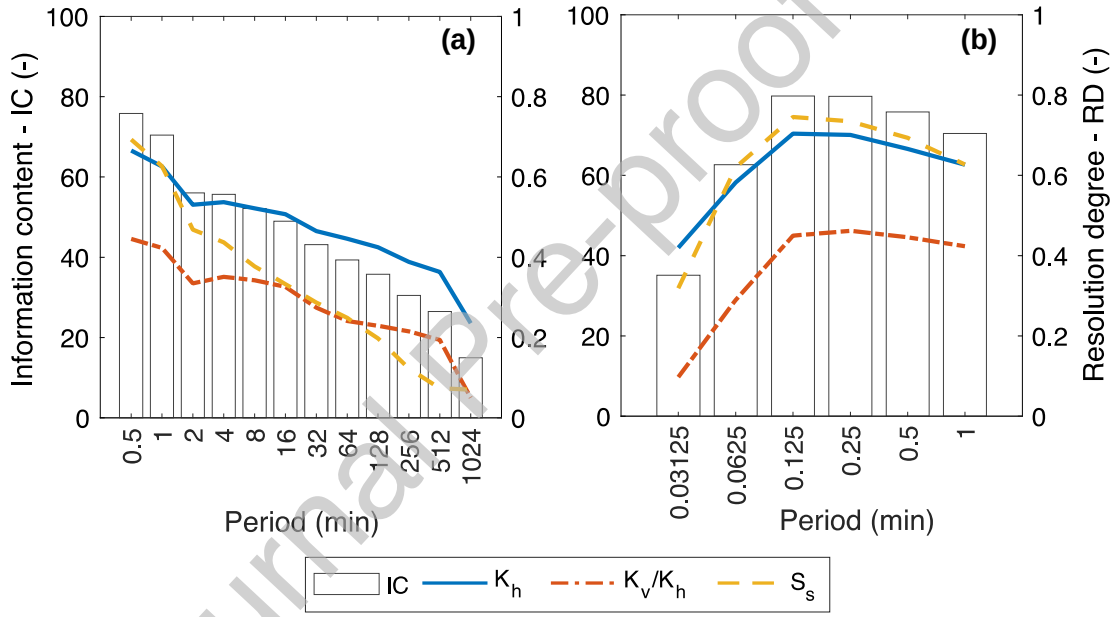

Figure 7. Change in total information content (*IC*) and resolution degree (*RD*) for each hydraulic property (K_h, K_v/K_h and S_s) with periods (a) for the base case with fixed peak amplitude A_0 (Simulations 1 in Tables 1 and 2) and (b) for additional periods shorter than those of the base case. Statistics apply to the cells within the focus area (Figure 1).

Figure 8 illustrates the spatial resolution of the hydraulic properties for three selected periods from Figure 7a by assigning the diagonal elements of the resolution matrix to the corresponding cells of

the parameter grid. While the magnitude of resolution decreases with increasing period, the resolution patterns for the three periods are similar. The higher resolution values for all hydraulic properties and periods are centered on the source well. Elsewhere on the parameter grid, the parameters for K_h are better resolved for cells immediately upstream and downstream of the observation well, while the parameters for K_v/K_h and S_s are better estimated for cells at the observation well itself. As noted in Figure 7a, the decrease in resolution for S_s is much more important with increasing period. There are other approaches (e.g. discrepancy principle, cross-validation) than the L-curve method to assess resolution, and their application would obviously yield somewhat different absolute resolution values. This is because a different basis of comparison is used. However, the general trend would be similar to those shown here.

It is noteworthy that the comparison of Figure 8 with Figure 6 shows that S_s is better resolved for the period with the higher sensitivities. However, for K_h and K_v/K_h, the higher resolution value is at sensitivity values below their maximum. The relationship between the sensitivities (magnitude and correlation) and the period leading to better resolution therefore varies depending on the hydraulic property under consideration.

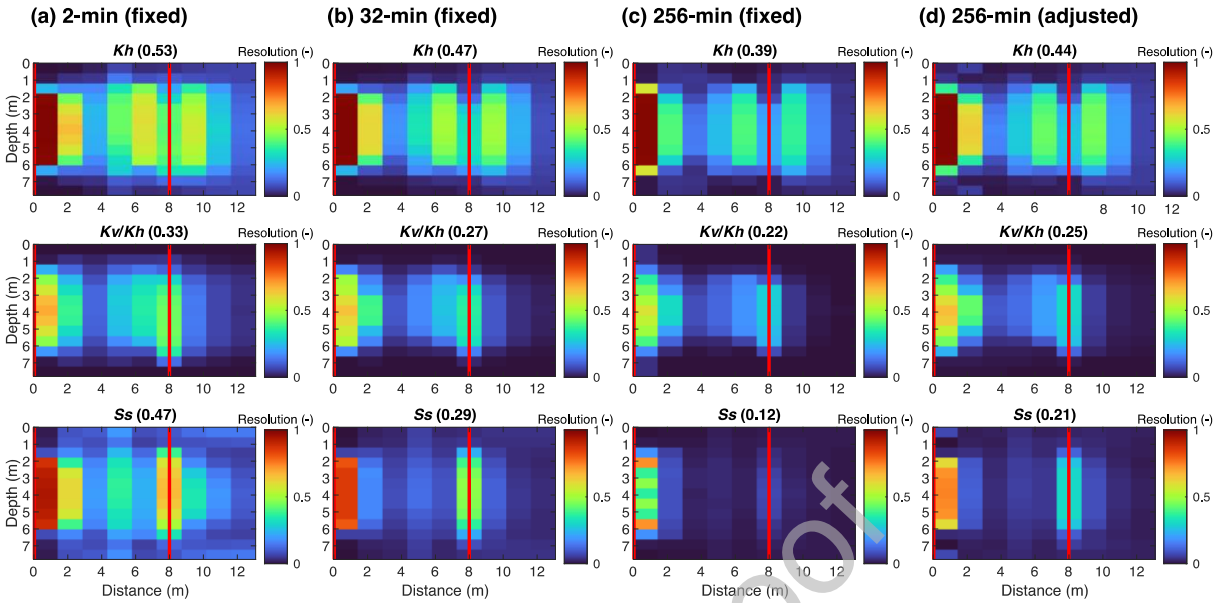

Figure 8. Spatial distribution of the resolution for the hydraulic properties K_h, K_v/K_h and S_s with the test strategy with fixed source signal magnitude A_0 for three selected periods: (a) 2 min; (b) 32 min; and (c) 256 min, and (d) 256-min with the test strategy with variable A_0. The resolution is evaluated for the head in the source and the observation intervals. The number in the parenthesis next to the name of the hydraulic property is the resolution degree (RD) within the focus area.

3.3 Adjusted A_0 to increase head and resolution for long periods

It has just been shown that the head variation for the source and observation intervals decreases for the longer periods, which may affect the resolution due to the low signal-to-noise ratio. To increase the head variation in the observation intervals, another test strategy is to adjust A_0 so that the head variation in the source interval remains the same for all periods (adjusted A_0 test strategy; Simulations 2 in Tables 1 and 2). With this strategy, a comparison of Figure 9 and Figure 3 shows that the head variations in the observation interval increase significantly for periods longer than 32 min. The head variations also reach a plateau for the longest periods. The heads in the observation intervals with the adjusted A_0 strategy are determined only by the degree of attenuation associated

with each period (Figure 10). As the comparison of Figure 6c and Figure 6d shows, a larger volume of the aquifer is investigated in this test strategy with long periods, as the head can be monitored at a greater distance from the source well.

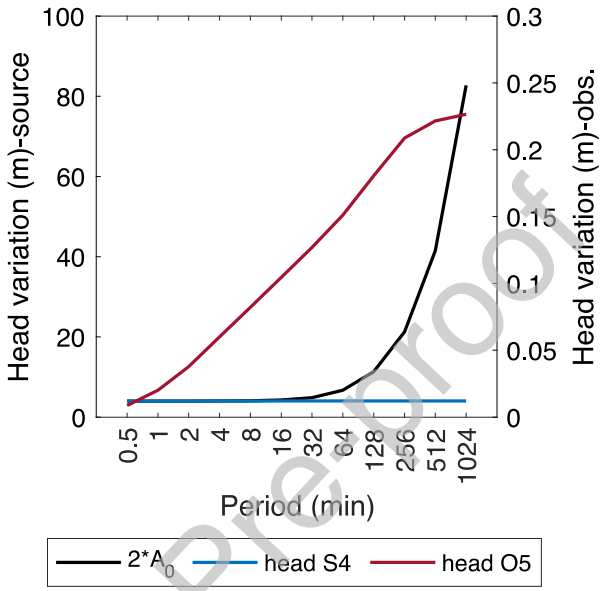

Figure 9. Example results obtained for the 2nd set of simulations for the variation of head in a source (S4) and an observation interval (O5) for twelve selected periods, using the same hydraulic properties as the base case but with the adjusted peak amplitude A_0 test strategy (Simulations 2 in Tables 1 and 2).

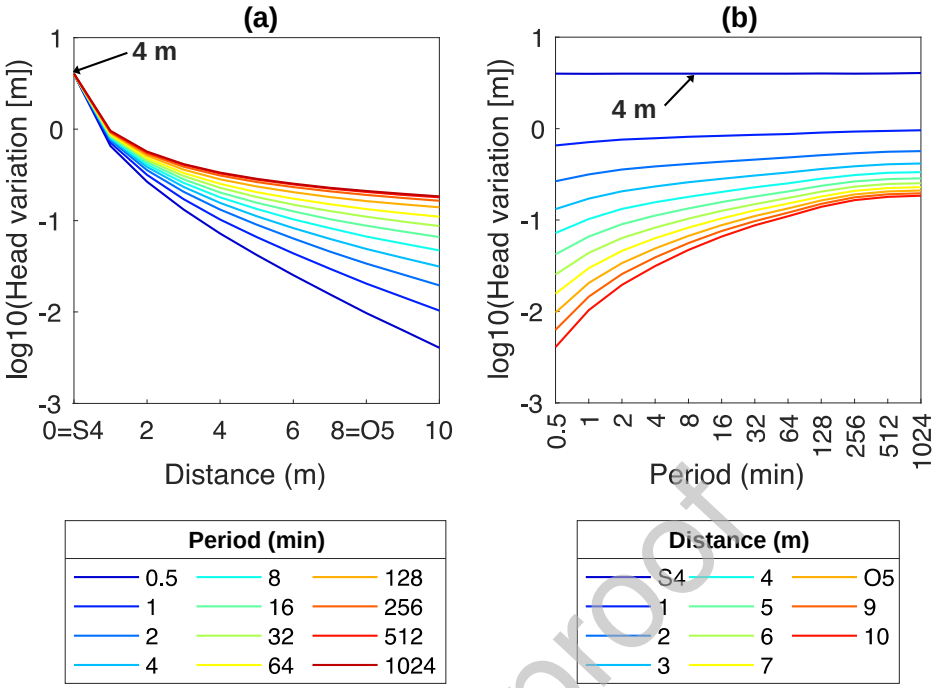

Figure 10. Variation of head with (a) distance from source interval for different periods and (b) period for different distances for the 2nd set of simulations with periodic tests with the adjusted peak amplitude A_0 strategy (Simulations 2 in Tables 1 and 2). The locations of the source (S4) and observation (O5) intervals are shown in Figure 1.

Figure 11 shows the same general downward trend in parameter resolution with period as in Figure 7a, but with slightly improved resolution for the longer periods. This is also clear from the comparison of Figures 8c and 8d. We can assume that the increased signal-to-noise ratio improved the resolution. However, even with much larger heads and a larger support volume, the longer periods are not as efficient as the shortest periods in reducing the correlation between parameter sensitivities.

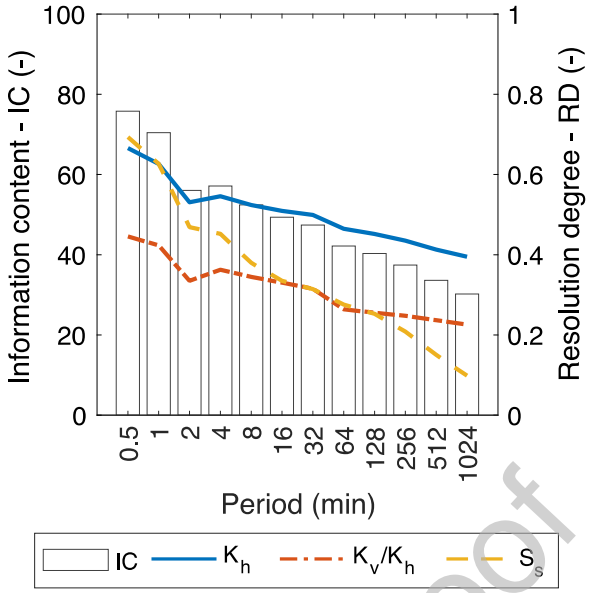

Figure 11. Change in information content (*IC*) and resolution degree (*RD*) for each hydraulic property (K_h, K_v/K_h and S_s) with period for the base case using the adjusted peak amplitude A_0 test strategy (Simulations 2 in Tables 1 and 2). Statistics are for cells within the focus area (Figure 1).

3.4 Importance of the transient phase

When a stationary column of water in a well is subjected to a periodic stress, the heads in the well and aquifer go through a transient phase before reaching a steady-periodic phase. The steady-periodic phase is reached when the difference between the extreme values of the head stabilizes (Figure 12). During the transient phase, the minima and maxima differ from the steady-periodic phase extremes (lower or higher). This section examines the resolution associated with these two phases. This analysis is performed with simulations using the adjusted A_0 test strategy (Simulations 2 in Tables 1 and 2).

Figure 12 shows that the difference in heads between the transient and steady state phases and the number of cycles of the transient phase vary with the period for both the source and observation

intervals. This can be explained by the relative magnitude of the flow injected or pumped into the source interval in relation to the capacity of the aquifer to store and transmit water. When the flow in the source well is greater than the capacity of the aquifer to receive it (Figures 12a and 12b), an overpressure head builds up in the source well and then propagates through the aquifer. On the other hand, when flow is low, transient heads are reduced due to storage allowed by the aquifer solid skeleton (Figures 12c and 12d). Figure 12 also shows that the absolute delay in time between the peak amplitudes of the source and the observation intervals increases with increasing period. This is consistent with the theory of tidal signal propagation in aquifers [7]. More importantly, the absolute delay in relation to the length of the period, i.e., the relative delay, increases with decreasing period. The longer the relative delay or the shorter the period, the less coherent is the movement of water in the aquifer. Therefore, the larger differences in associated spatial and temporal sensitivities improve parameter resolution for the shorter periods.

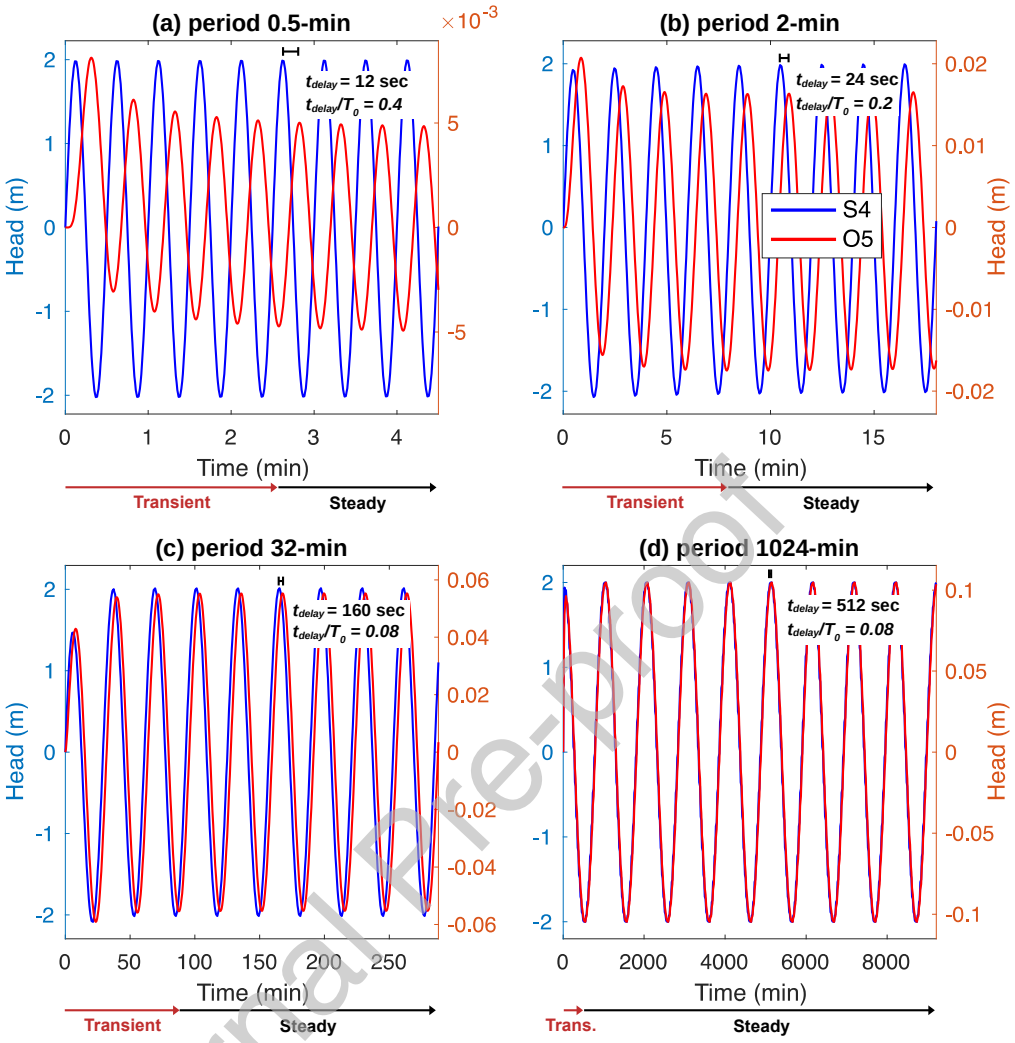

Figure 12. Examples of the heads at a source interval (S4) and an observation interval (O5) for the transient and steady-periodic phases for four selected periods: (a) 0.5 min; (b) 2 min; (c) 32 min; and (d) 1024 min. The acronyms t_{delay} and t_{delat}/T_0 stand for the absolute and relative time delay between the source and the observation intervals, respectively, where T_0 is the period. Results refer to the adjusted peak amplitude A_0 test strategy (Simulations 2 in Tables 1 and 2).

The information content for various combinations of cycles for a range of periods between 0.5 and 1024 min is shown in Figure 13. The information content of the first two transient cycles is higher

than that of the subsequent cycle combinations at or near steady-periodic state (cycles 3-4, 5-6, and 7-8). The difference is more pronounced for the shorter periods with stronger transient effects. Moreover, the resolution obtained with only the transient cycles (cycles 1-2) is equal to or higher than the resolution estimated in Figure 11 for the first six cycles. These results show that all the information about the hydraulic properties is contained in the transient phase.

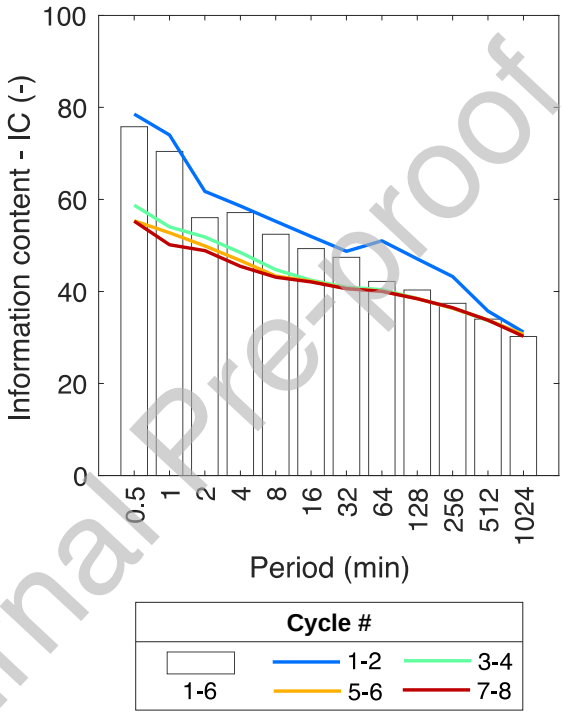

Figure 13. Information content (*IC*) with period associated with resolution analysis using various combinations of periodic cycles. Cycles 1-2 and 7-8 are most representative of the transient and steady-periodic phase, respectively. The scenario with cycles 1-6 is the same as shown in Figure 11. Results refer to the adjusted peak amplitude A_0 test strategy (Simulations 2 in Tables 1 and 2).

Figure 14 also compares the resolution degree for the three hydraulic properties (K_h, K_v/K_h and S_s) for the transient phase (cycles 1-2) and the steady state phase (cycles 7-8). While there is a strong decreasing trend in the resolution with period for all hydraulic properties of the transient phase, the trend for the steady-periodic phase is much less pronounced (except Ss). The resolution values for each period of the transient phase are higher than those of the steady-periodic phase.

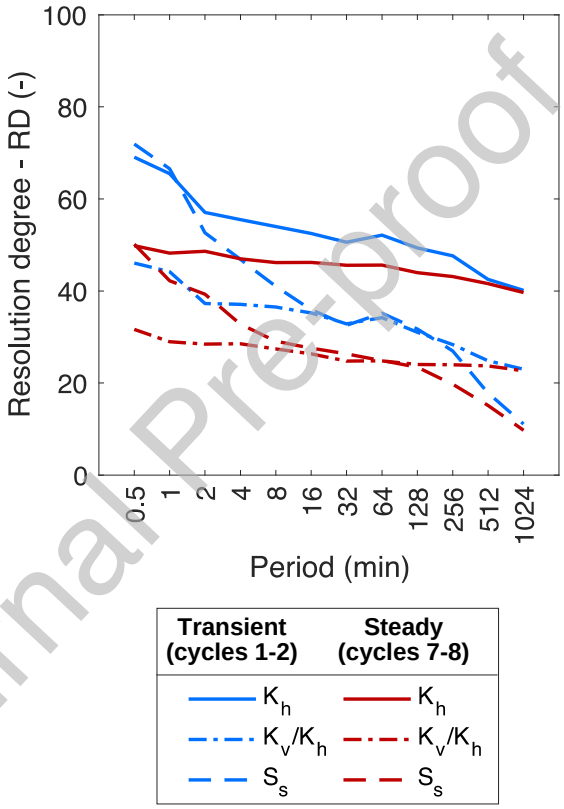

Figure 14. Resolution degree (*RD*) with period for each hydraulic property (K_h, K_v/K_h and S_s) for the transient (cycles 1-2) and the steady-periodic phase (cycles 7-8). Results refer to the adjusted peak amplitude A_0 test strategy (Simulations 2 in Tables 1 and 2).

3.5 Benefit of combining multiple periods

This section examines the benefits of combining multiple periods. Since tests with different periods yield different sensitivity patterns (e.g. Figure 6), combining them should improve resolution. For this analysis, the sensitivities obtained for tomographic experiments with different periods are first combined and then the resolution associated with the combined sensitivity matrix is evaluated. All non-redundant combinations with 2, 3 and 4 periods are tested. A total of 6 cycles is considered for each tomographic experiment.

Figure 15 shows the two best combinations with the highest information content for each combination scenario (1, 2, 3 and 4 periods). It is clear that combining multiple periods slightly improves the resolution compared to using a single period. The improvement is slightly greater with the adjusted A_0 test strategy. In the two test strategies, the best combination always includes the shortest period (0.5 min), often with the next shortest period (1 min) and other much longer. The long periods are of longer duration in the adjusted A_0 test strategy, which is due to the recording of larger heads that significantly exceed the noise level. The increase in resolution through a combination of short periods was also reported by Ahn and Horne [25]. However, the results in Figure 15 also include long periods. For example, for the combination scenario with four periods in Figure 15b, the best resolution is for the combination with the two shortest periods (0.5 and 1 min) with two long periods (256 and 1024 min). This shows that the different sensitivity patterns associated with the different period lengths complement each other to resolve the hydraulic parameters, as previously suggested by Cardiff et al [26].

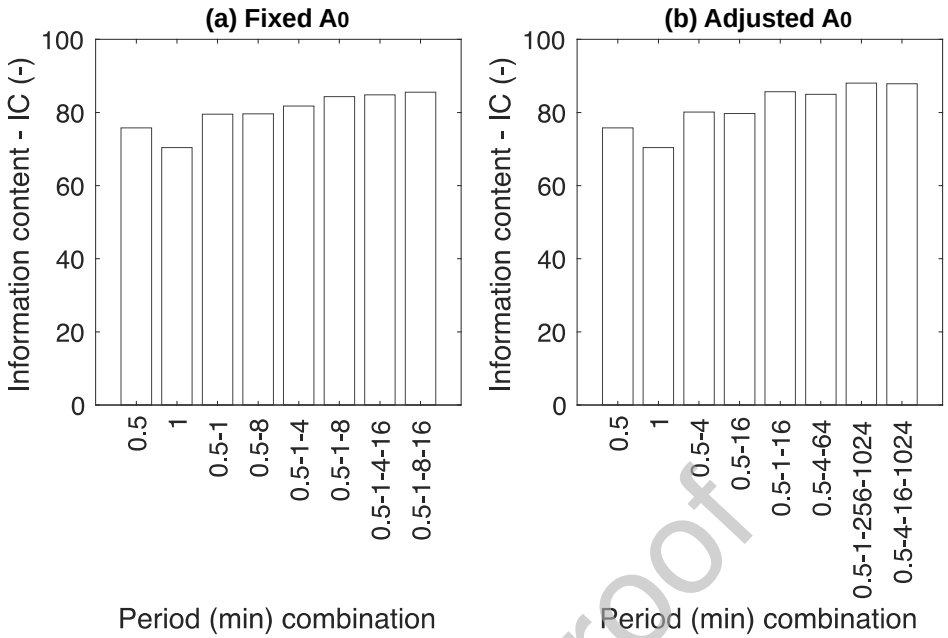

Figure 15. Comparison of information content (*IC*) for different combinations of periods for periodic tests with: (a) fixed peak amplitude A_0 (Simulations 1 in Tables 1 and 2) and (b) adjusted A_0 with period (Simulations 2 in Tables 1 and 2). (a) and (b) show the two best resolutions for each period combination. The total number of combinations tested is 66, 220, and 495 using 2, 3, and 4 periods, respectively.

3.6 Influence of the hydraulic parameters

Using a fixed A_0 test strategy, the third set of simulations (Simulations 3 in Tables 1 and 2) explored the effect of different values of hydraulic parameters. Figures 16, 17 and 18 show the influence of K_h, K_v/K_h and S_s, respectively, on the head and resolution. The values of the hydraulic properties are increased and decreased by a factor of four compared to the base case (Simulations 1), while all other parameters remain identical. Note that the same twelve periods are simulated as for the base case, except for the K_h scenarios, where the shortest and longest periods have been adjusted to account for the dependence of the maximum head on K_h (see below).

Figures 16a, 17a, and 18a show that both K_v/K_h and S_s affect the head for the period of maximum head variation. At lower K_v/K_h, the head in the observation interval increases due to concentrated flow in the horizontal plane of the source interval (O5 in Figure 19b). Outside this plane, the head is lower due to decreased vertical flow (O6 in Figure 19b). As the aquifer approaches isotropy, the difference in head between points at any angle of observation becomes insignificant. For S_s, the head for the observation interval decreases with S_s as more water is stored in the aquifer.

Figures 16b, 17b, and 18b also show that only K_h influences the period in which the maximum head variation is reached in the observation interval. The effect of K_h on the heads is a general shift along the time axis, as is the period of maximum head variation. This period shift is inversely proportional to K_h (e.g., doubling K_h decreases the period by a factor of 2).

Finally, Figures 16c, 17c, and 18c show that the information content at the period of maximum head is similar for all scenarios. However, the maximum resolution is higher at lower K_v/K_h and higher S_s. The better resolution at lower K_v/K_h is explained by the fact that anisotropy increases the contrast of vertical hydraulic gradients in the aquifer (e.g., the difference between O5 and O6 in Figure 19b), which leads to different sensitivity patterns. The heads are also higher for better signal-to-noise ratios. On the other hand, a higher S_s value is associated with a more pronounced transient response of the head at early times (Figure 19c). We note that the head patterns for K_h are identical and only the period differs, which explains a similar resolution for the simulated range of K_h values (Figure 19a). The difference in magnitude and trend of information content between the periods of maximum head variation and maximum resolution is due to the more important transient behavior for the shorter periods (e.g., Figure 12). The period of 0.5 min has the maximum information

content for all scenarios, except for the lower and higher K_h scenarios, for which periods of 0.125 and 8 min have better resolution, respectively.

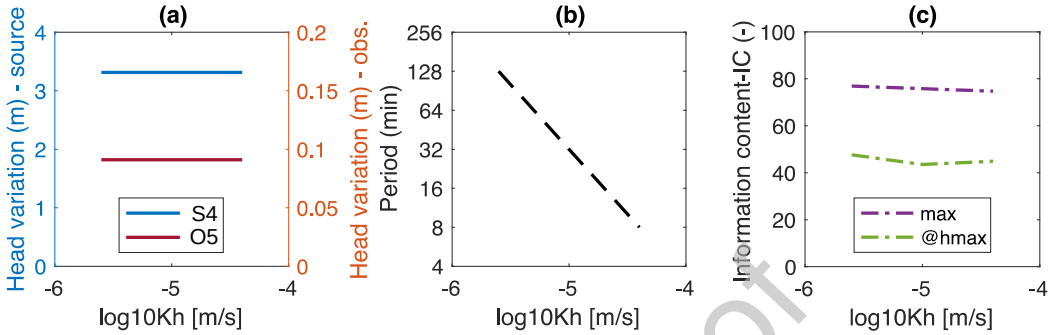

Figure 16. Influence of K_h (Simulations 3 with fixed A_0 test strategy, Tables 1 and 2). (a) Head variation in the source and observation intervals for the period for which the maximum head variation is reached in the observation interval (e.g., Figure 3). (b) The period of maximum head variation in the observation interval. (c) The information content (*IC*) for the periods of maximum head variation (@hmax) and maximum resolution (max).

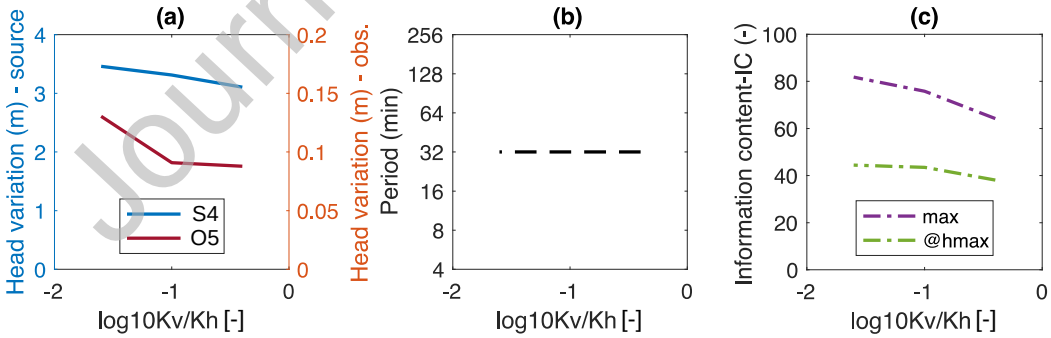

Figure 17. Influence of K_v/K_h (Simulations 3 with fixed A_0 test strategy, Tables 1 and 2). (a) Head variation in the source and observation intervals for the period for which the maximum head variation is reached in the observation interval. (b) The period of maximum head variation in the

observation interval. (c) The information content (*IC*) for the periods of maximum head variation (@hmax) and maximum resolution (max).

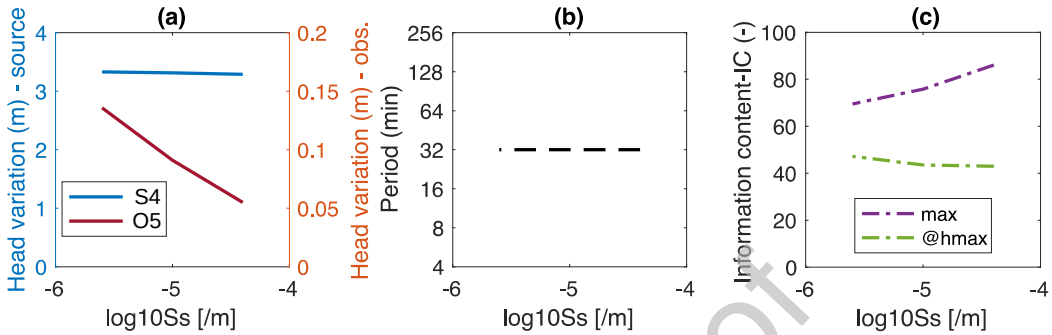

Figure 18. Influence of S_s (Simulations 3 with fixed A_0 test strategy, Tables 1 and 2). (a) Head variation in the source and observation intervals for the period for which the maximum head variation is reached in the observation interval. (b) The period of maximum head variation in the observation interval. (c) The information content (*IC*) for the periods of maximum head variation (@hmax) and maximum resolution (max).

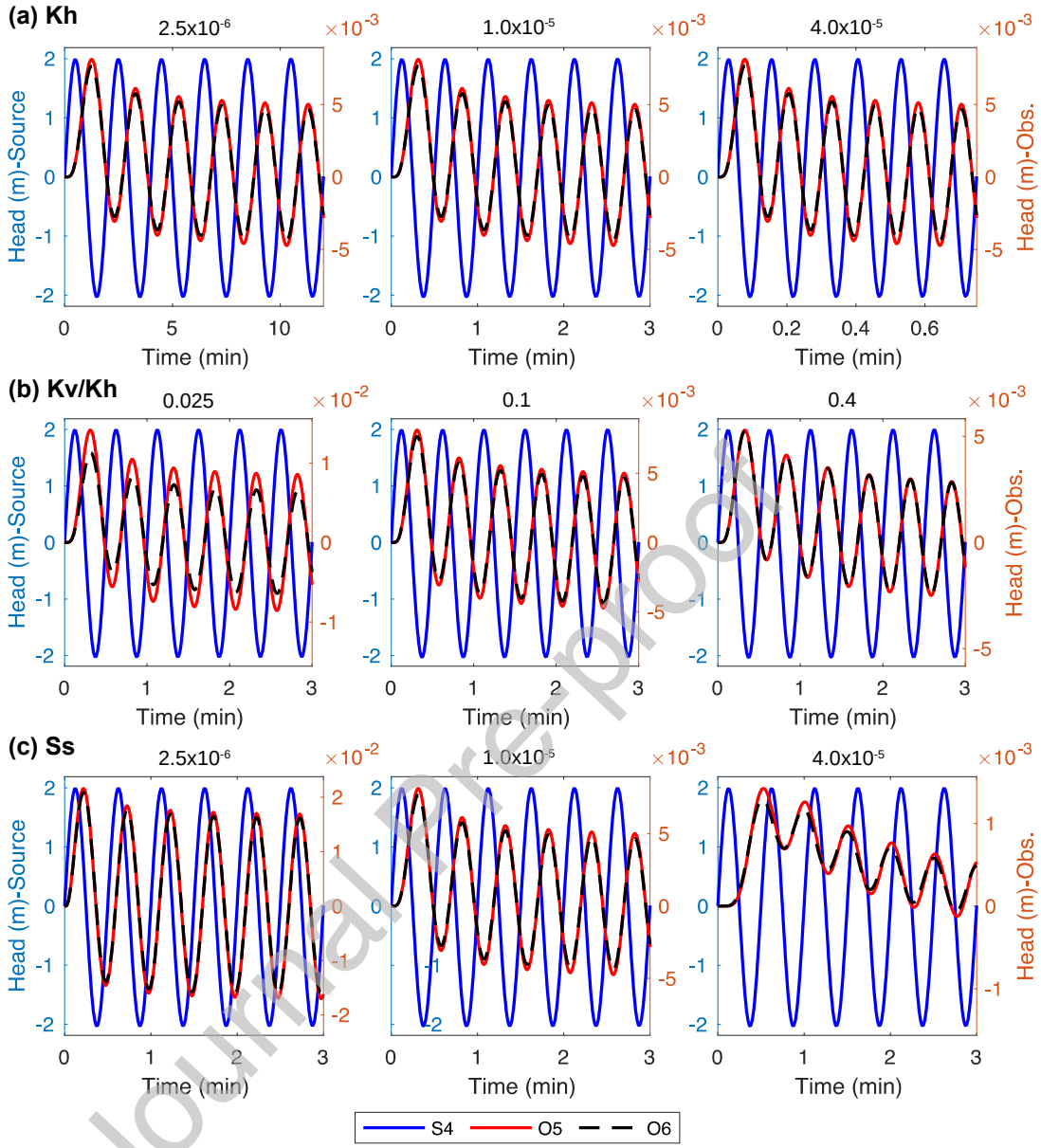

Figure 19. Simulated head for one source interval (S4) and two observation intervals (O5 and O6) for different values of: (a) K_h; (b) K_v/K_h; and (c) S_s for the period of maximum resolution. Results are for Simulations 3 with a fixed A_0 test strategy (Tables 1 and 2). The locations of S4, O5 and O6 are shown in Figure 1.

3.7 Influence of the source

The 4th and 5th set of simulations (Tables 1 and 2) are done to investigate how the test conditions related to the magnitude of the peak amplitude (A_0) and the ratio of the casing and well radii (r_c/r_w) affect the heads and resolutions, respectively. As expected, Figure 20a shows that increasing A_0 leads to higher heads in the source and observation intervals. However, the period of maximum head is not affected (Figure 20b) because the relative flux and gradients between periods are similar for all A_0 scenarios. Resolutions also increase slightly with A_0 (Figure 20c) due to a better signal-to-noise ratio (Figure 21a). The maximum information content is for the period of 0.5 min for all A_0 scenarios.

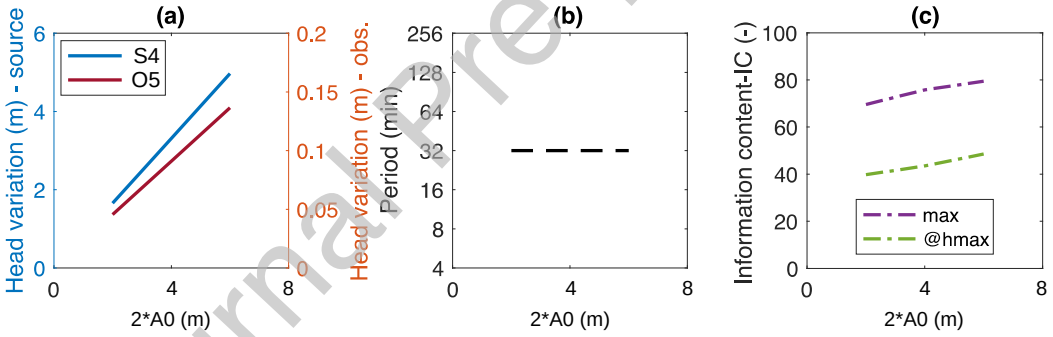

Figure 20. Influence of the magnitude of the peak amplitude A_0 for Simulations 4 with a fixed A_0 test strategy (Tables 1 and 2). (a) Head variation in the source and observation intervals for the period in which the maximum head variation is reached in the observation interval. (b) The period of maximum head variation in the observation interval. (c) The information content for the periods of maximum head variation (@hmax) and maximum resolution (max).

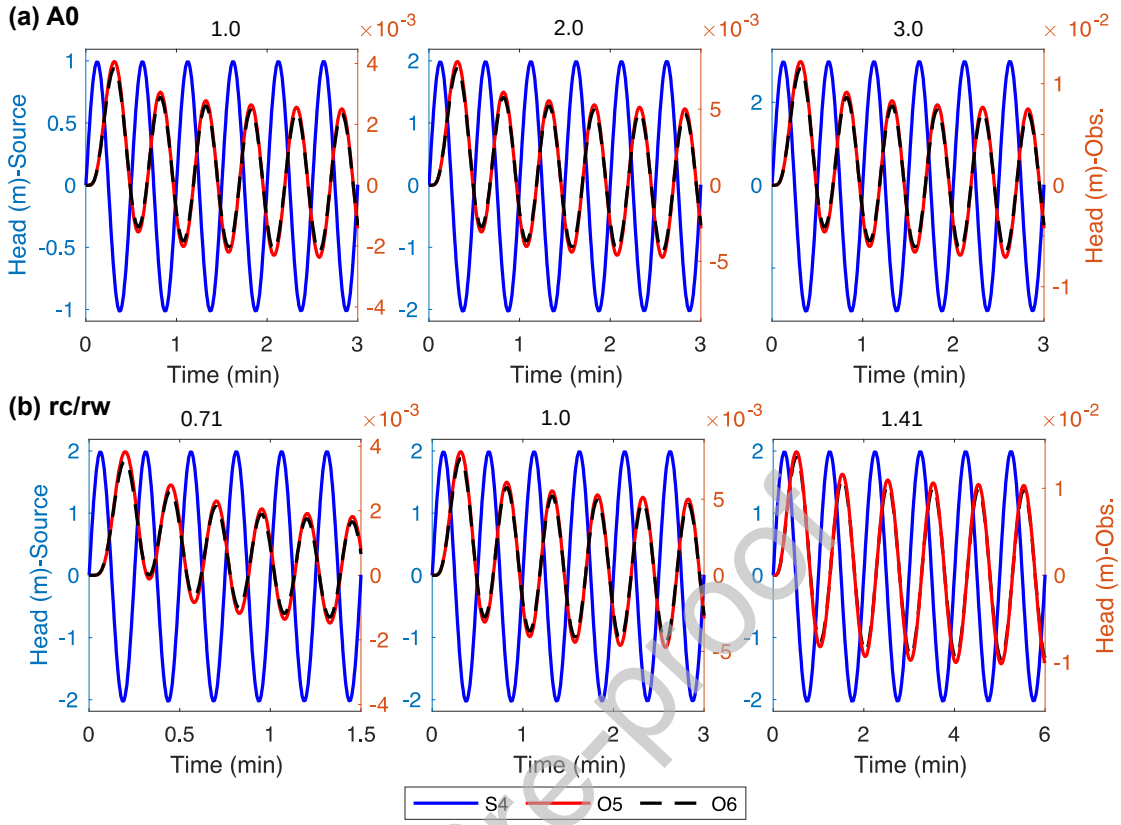

Figure 21. Simulated head for one source interval (S4) and two observation intervals (O5 and O6) for different values of: (a) A_0 (Simulations 4); and (b) r_c/r_w (Simulations 5) for the period of maximum resolution. The fixed A_0 test strategy is simulated. The locations of S4, O5 and O6 are shown in Figure 1.

Figure 22a shows that an increase in r_c/r_w leads to higher heads in the observation interval (and very slightly in the source interval). That is, larger r_c/r_w values increase the flow in the source interval, while the hydraulic gradient between the source well and the aquifer remains almost the same. Consequently, for the same capacity of the aquifer, the period of maximum head variation is longer to compensate for the greater flow (Figure 22b). The increase of the period is proportional to the square root of r_c/r_w.

Resolution is not significantly affected by r_c/r_w (Figure 22c). While transient behavior is more important at lower r_c/r_w and should result in better resolution, this may be offset by a weaker signal-to-noise ratio (Figure 21b). The periods of maximum information are 0.25, 0.5, and 1 min for the lower, base, and higher r_c/r_w scenarios, respectively.

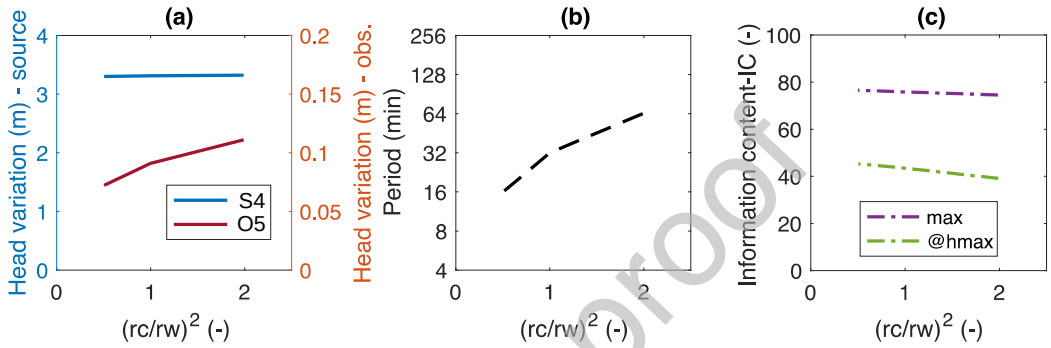

Figure 22. Influence of the ratio of the casing and well radii r_c/r_w for Simulations 5 with a fixed A_0 test strategy (Tables 1 and 2). (a) Head variation in the source and observation intervals for the period in which the maximum head variation is reached in the observation interval. (b) The period of maximum head variation in the observation interval. (c) The information content for the periods of maximum head variation (@hmax) and maximum resolution (max).

4 Conclusions

To the authors' knowledge, this study is the first to quantitatively assess the information content of heads generated by periodic signals in wells to characterize the spatial resolution of K_h, K_v/K_h and S_s of aquifers. A numerical framework combining groundwater flow simulation and resolution analysis was used for this assessment. The numerical groundwater flow model, which accounts for storage in the source well, was used to represent a series of hydraulic tests with different periods between a source well and an observation well. Small intervals along the wells were considered, such as those obtained with packers in a tomography configuration. The heads in the intervals were simulated and the sensitivity of these heads to hydraulic properties discretized over small cells was evaluated with the model by perturbation. The resolution analysis using the sensitivity matrix of the simulated tomographic experiments was based on the L-curve criteria for a clear separation between noise amplification and parameter resolution. This approach made it possible to compare tomographic experiments with different periods on a common basis.

The most important contributions of this study are summarized below.

1) A better resolution is achieved if the transient phase is considered. It has been shown that all information about the hydraulic properties is contained in the first cycles of the periodic signal, where the effects of transient behavior are greatest. Later cycles do not convey any more information beyond that contained in the earlier cycles and convey less information themselves. This is consistent with Copty and Findikakis [57] who stated that “the statistical spatial structure of the transmissivity field can potentially be determined from the transient drawdown rate of the heterogeneous system.” Furthermore, the resolution is better for the shorter periods where the

transient effects are largest. The sharper hydraulic gradients produced reduce the correlation between the sensitivities better. However, there is a practical minimum length for the period that must not be exceeded. As the head penetration distance is less important for short periods, the head in the observation wells can no longer be distinguished from the noise level and the resolution deteriorates. The period for optimal resolution is also related to K_h, with shorter periods required for permeable aquifers. This result is in contrast to previous studies, which generally only consider the steady-periodic phase of the signal in their analysis [e.g. 8,9,10,11,12,13,14,15,16,17,18,19,20,21,22,23,24,25,26,27]. In practice, this result also implies that fieldwork duration can be reduced by using fewer cycles to achieve the maximum benefit.

2) There is a trade-off between spatial resolution and support volume. In general, increasing the test period allows the measurement of head variations at a greater distance from the source well and facilitates the estimation of hydraulic properties over a larger support volume. However, the increase of the support volume with the period leads to a lower spatial resolution. As the length of the period increases, the water displacement in the aquifer becomes more uniform, making it difficult to identify the individual contributions of the different aquifer regions to the head (resulting in highly correlated sensitivities). Therefore, shorter periods are more effective for mapping local heterogeneities (between wells), while longer periods are more suitable for estimating hydraulic properties over larger support volumes [5,6]. The difference in 'sensitivity maps' for different periods has already been shown by Cardiff et al [26], but this study highlights the associated spatial resolution.

3) The combination of several periods could increase the spatial resolution. This study showed that the combination of several periods slightly improves the resolution of the aquifer properties.

As a rule, the best combination of periods always includes of the shortest periods and much longer periods of medium to long length. The combination of periods does not lead to a systematic improvement and should therefore be chosen carefully. This could explain why Wang et al. [27] observed "that the estimates [of transmissivity] from different frequencies and multifrequency tests are indistinguishable on average". They used excessively long periods (e.g. 400 to 10800 minutes) for their analysis in relation to the transmissivity of the simulated aquifer. As this study has shown, long periods convey less information and their relative additional contribution is negligible, especially when only the steady-periodic phase is considered in the analysis. The weak contribution of long periods to the resolution of hydraulic properties was also reported by Anh and Horne [25], who stated that the exclusive use of "frequencies having radii [of influence] that extend beyond the observation well does not lead to a correct estimate [of permeability]". In contrast, Cardiff et al [26] have shown "that progressive improvement in aquifer imaging results can be obtained by then jointly inverting multiple frequencies' responses". They also used much shorter periods (e.g. 5 seconds to 5 minutes) for testing in a channel-type aquifer with a K_h contrast of one order between the channel and the matrix. Visually, the improvement in resolution by combining periods obtained by Cardiff et al [26] is more significant than what was obtained in this study with a homogeneous model. This could be due to the nature of the hydraulic property fields. The heterogeneous nature of the hydraulic properties can lead to strong contrasts in hydraulic gradients that reduce the correlation between parameters. Similar to this study, the increase in anisotropy (decrease in K_v/K_h value) led to an increase in resolution due to the greater contrast in head between the different intervals in the observation well. Another plausible cause is that Cardiff et al [26] only considered K_h in their analysis. When only one hydraulic property is considered, the correlation that exists between the other hydraulic properties (e.g. between K_h and S_s) is ignored. This leads to an improvement in resolution for the property under consideration. This agrees with Anh and Horne [25] who reported that "when porosity is another unknown, the permeability does

not match as well as in the constant porosity case". This suggests that the gain in combining periods could be case-specific, which would require further studies to better design periodic tests under field conditions.

4) Tomographic periodic tests can be used to estimate the vertical anisotropy of hydraulic conductivity. To better illustrate the general principles associated with periodic testing, the effects of heterogeneity have been intentionally omitted from the analysis, although scenarios with different homogeneous property values have been considered. However, it was shown that K_v/K_h, which expresses the effects of small-scale heterogeneity at a larger scale, can be resolved with periodic tests in a tomographic configuration. This is an important contribution as there are very few field methods for estimating K_v/K_h, (see 43 for a review). Cheng and Renner [14,58] already proposed periodic testing along a single well to estimate K_v/K_h, but this study extends the concept to multiple wells.

In summary, this study provides a comprehensive framework to understand the information contained in the heads generated by periodic tests. This framework made it possible to explain the results of previous studies that were seemingly contradictory by providing a broader context for their interpretation. It is hoped that with this new understanding, periodic tests can be better designed for use in the field. The need for accurate and effective field techniques to characterize aquifer systems cannot be overstated.

5 Acknowledgements

We thank two anonymous reviewers for their constructive comments to improve the clarity of the manuscript. We also thank Glenn Duffield for his technical support for AQTESOLV and Nicolas Benoit for his internal review of the paper. This is a GSC contribution 20230252.

6 References

[1] Butler, Jr. J.J., 2019. The Design, Performance, and Analysis of Slug Tests (2nd Edition). CRC Press, 266 pp.

[2] Kruseman, G.P. de Ridder, N.A., 2000. Analysis and Evaluation of Pumping Test Data (2nd Edition). International Institute for Land Reclamation and Improvement, 372 pp.

[3] Paradis, D., Lefebvre, R., Gloaguen, E., Giroux, B., 2016. Comparison of slug and pumping tests for hydraulic tomography experiments: a practical perspective. Environmental Earth Sciences, 75: 1159, 10.1007/s12665-016-5935-4

[4] Butler, Jr J.J., McElwee, C.D., 1990. Variable-rate pumping tests for radially symmetric nonuniform aquifers. Water Resources Research, 26(2): 291-306

[5] Black, J.H., Kipp, K.L.J., 1981. Determination of hydrogeological parameters using sinusoidal pressure tests: A theoretical appraisal. Water Resources Research, 17(3): 686–692, 10.1029/WR017i003p00686

[6] Hollaender, F., Hammond, P.S., Gringarten, A.C., 2002. Harmonic testing for continuous well and reservoir monitoring. In Proceedings - SPE Annual Technical Conference and Exhibition, (pp. 3071–3082). San Antonio, TX: Society of Petroleum Engineers (SPE), 10.2118/77692-MS

[7] Ferris, J.G., 1952. Cyclic fluctuations of water level as a basis for determining aquifer transmissibility. United States Geological Survey, Washington, D.C. 16 pp. doi.org/10.3133/70133368

[8] Rasmussen, T.C., Haborak, K.G., Young, M.H., 2003. Estimating aquifer hydraulic properties using sinusoidal pumping at the Savannah River site, South Carolina, USA. Hydrogeology Journal 11(4): 466–482, 10.1007/s10040-003-0255-7

[9] Nakao, S., Ishido, T., Hatakeyama, K., Ariki, K., 2005. Analysis of Pulse Tests in a Fractured Geothermal Reservoir-Case Study at the Sumikawa Field in Japan. In: Proceedings World Geothermal Congress, Antalya, Turkey, 24–29 April 2005

[10] Renner, J., Messar, M., 2006. Periodic pumping tests. Geophysical Journal International 167(1): 479–493, 10.1111/j.1365-246X.2006.02984.x

[11] Becker, M.W., Guiltinan, E., 2010. Cross-hole periodic hydraulic testing of inter-well connectivity. In: Thirty-Fifth Workshop on Geothermal Reservoir Engineering. Stanford University, Stanford, California

[12] Rabinovich A., W. Barrash, M. Cardiff, D.L. Hochstetler, T. Bakhos, G. Dagan, P.K. Kitanidis. 2015. Frequency dependent hydraulic properties estimated from oscillatory pumping tests in an unconfined aquifer. Journal of Hydrology 531: 2-16.

[13] Guiltinan, E., Becker, M.W., 2015. Measuring well hydraulic connectivity in fractured bedrock using periodic slug tests. Journal of Hydrology 521: 100–107, 10.1016/j.jhydrol.2014.11.066

[14] Cheng, Y., Renner, J., 2018. Exploratory use of periodic pumping tests for hydraulic characterization of faults. Geophysical Journal International, 212(1): 543–565, 10.1093/gji/ggx390

[15] Sayler, C., Cardiff, M., Fort, M.D., 2018. Understanding the geometry of connected fracture flow with multiperiod oscillatory hydraulic tests. Groundwater 56(2): 276–287

[16] Fokker, P.A., Renner, J., Verga, F., 2013. Numerical modeling of periodic pumping tests in wells penetrating a heterogeneous aquifer, Am. J. Environ. Sci., 9, 1–13.

[17] Cardiff, M., Bakhos, T., Kitanidis, P.K., Barrash, W., 2013. Aquifer heterogeneity characterization with oscillatory pumping: Sensitivity analysis and imaging potential. Water Resources Research, 49: 5395–5410, 10.1002/wrcr.20356

[18] Lavenue, M., deMarsily, G., 2001. Three-dimensional interference test interpretation in a fractured aquifer using the Pilot Point Inverse Method. Water Resour. Res. 37 (11), 2659–2675. https://doi.org/10.1029/2000WR000289.

[19] McElwee, C.D., Engard, B.R., Wachter, B.J., Lyle, S.A., Healey, J., Devlin, J.F., 2011. Hydraulic tomography and high-resolution slug testing to determine hydraulic conductivity distributions, Kansas Geol. Surv. Open File Rep., p. 168.

[20] Fokker, P.A., Salina Borello, E., Serazio, C., Verga, F., 2012. Estimating reservoir heterogeneities from pulse testing. J. Petrol. Sci. Eng. 86–87, 15–26. dx.doi.org/10.1016/j.petrol.2012.03.017.

[21] Fischer P., Jardani, A., Jourde, H., Cardiff, M., Wang, X., Chedeville, S., Lecoq, N., 2018. Harmonic pumping tomography applied to image the hydraulic properties and interpret the connectivity of a karstic and fractured aquifer (Lez aquifer, France). Advances in Water Resources,119: 227-244. https://doi.org/10.1016/j.advwatres.2018.07.002

[22] Fischer, P., De Clercq, T., Jardani, A., Massei, N., Abbas, M., 2020. Imaging the hydraulic properties of a contaminated alluvial aquifer perturbed with periodic signals. Hydrogeol J 28, 2713–2726, doi.org/10.1007/s10040-020-02233-8

[23] Cardiff, M., Zhou, Y., Barrash, W., Kitanidis, P.K., 2020. Aquifer imaging with oscillatory hydraulic tomography: Application at the field scale. Groundwater 58(5): 710–722, 10.1111/gwat.12960

[24] Rosa, A.J., Horne, R.N., 1997. Reservoir description by well-test analysis by use of cyclic flow-rate variation. SPE Formation Evaluation, 12(04), 247–254, 10.2118/22698-PA

[25] Ahn, S., Horne, R.N., 2010. Estimating permeability distributions from pressure pulse testing. In Proceedings - SPE Annual Technical Conference and Exhibition, 3:2388–2403. Florence, 10.2118/134391-MS

[26] Cardiff, M., Bakhos, T., Kitanidis, P.K., Barrash, W., 2013. Aquifer heterogeneity characterization with oscillatory pumping: Sensitivity analysis and imaging potential. Water Resources Research 49, no. 9: 5395–5410. doi.org/10.1002/wrcr.20356

[27] Wang, Y.-L., Yeh, T.-C.J., Xu, D., Li, K., Wen, J.-C., Huang, S.-Y., Wang, W., Hao, Y., 2021. Stochastic analysis of oscillatory hydraulic tomography. Journal of Hydrology, 596, 10.1016/j.jhydrol.2021.126105

[28] Li, H., Jiao, J.J., 2001. Analytical studies of groundwater-head fluctuation in a coastal confined aquifer overlain by a semi-permeable layer with storage. Advances in Water Resources, 24(5): 565-573, 10.1016/S0309-1708(00)00074-9

[29] Chuang, M.H., Yeh, H.D., 2007. An analytical solution for the head distribution in a tidal leaky confined aquifer extending an infinite distance under the sea. Advances in Water Resources, 30(3), 439-445, 10.1016/j.advwatres.2006.05.011

[30] Guarracino, L., Carrera, J., Vázquez-Suñé, E., 2012. Analytical study of hydraulic and mechanical effects on tide-induced head fluctuation in a coastal aquifer system that extends under the sea. Journal of Hydrology, 450–451, 150-158, 10.1016/j.jhydrol.2012.05.015

[31] Fuentes-Arreazola, M.A., Ramírez-Hernández, J., Vázquez-González, R., 2018. Hydrogeological properties estimation from groundwater level natural fluctuations analysis as a low-cost tool for the Mexicali Valley Aquifer. Water, 10, 586, 10.3390/w10050586

[32] Bakker, M., 2019. Analytic solutions for tidal propagation in multilayer coastal aquifers. Water Resources Research, 55, 3452–3464, 10.1029/2019WR024757

[33] Srzić, V., Lovrinović, I., Racetin, I., Pletikosić, F., 2020. Hydrogeological characterization of coastal aquifer on the basis of observed sea level and groundwater level fluctuations: Neretva Valley Aquifer, Croatia. Water, 12, 348, 10.3390/w12020348

[34] Aster, R.C., Borchers, B., Thurber, C.H., 2005. Parameter Estimation and Inverse Problems. Elsevier, Amsterdam, 301 pp.

[35] Bohling, G.C., Butler Jr. J.J., 2001. lr2dinv: a finite-difference model for inverse analysis of two-dimensional linear or radial groundwater flow. Comput. Geosci. 27 (10), 1147–1156.

[36] Bohling., G.C., Zhan, X., Butler, J.J.Jr., Zheng, L., 2002. Steady shape analysis of tomographic pumping tests for characterization of aquifer heterogeneities. Water Resources Research, 38(12), 10.1029/2001WR001176

[37] Bohling, G.C., Butler, J.J.Jr., Zhan, X., Knoll, M.D., 2007. A field assessment of the value of steady shape hydraulic tomography for characterization of aquifer heterogeneities. Water Resources Research, 43(5), 10.1029/2006WR004932

[38] Liu, G., Bohling, G.C., Butler, J.J.Jr., 2008. Simulation assessment of the direct-push permeameter for characterizing vertical variations in hydraulic conductivity. Water Resources Research, 44(2), 10.1029/2007WR006078

[39] Bohling, G.C., 2009. Sensitivity and resolution of tomographic pumping tests in an alluvial aquifer. Water Resources Research, 45(2), 10.1029/2008WR007249

[40] Liu, G., Butler, J.J.Jr., Bohling, G.C., Reboulet, E.C., Knobbe, David, S., Hyndman, W., 2009. A new method for high-resolution characterization of hydraulic conductivity. Water Resources Research, 45(8), 10.1029/2009WR008319

[41] Bohling, G.C., Liu, G., Knobbe, S., Reboulet, E.C., Hyndman, D.W., Dietrich, P., Butler, J.J.Jr., 2012. Geostatistical analysis of centimeter-scale hydraulic conductivity variations at the MADE site. Water Resources Research, 48(2), 10.1029/2011WR010791

[42] Zschornack, L., Bohling, G.C., Butler, J.J.Jr., Dietrich, P., 2013. Hydraulic profiling with the direct-push permeameter: Assessment of probe configuration and analysis methodology. Journal of Hydrology, 496:195-204, 10.1016/J.JHYDROL.2013.05.036

[43] Paradis, D., Lefebvre, R., 2013. Single-well interference slug tests to assess the vertical hydraulic conductivity of unconsolidated aquifers. Journal of Hydrology, 478: 102-118, 10.1016/J.JHYDROL.2012.11.047

[44] Paradis, D. Gloaguen, E., Lefebvre, R., Giroux, B., 2015. Resolution analysis of tomographic slug test head data: Two-dimensional radial case. Water Resources Research, 51(4): 2356-2376, 10.1002/2013WR014785

[45] Paradis, D., Gloaguen, E., Lefebvre, R., Giroux, B., 2016. A field proof-of-concept of tomographic slug tests in an anisotropic littoral aquifer. Journal of Hydrology, 536:61-73, 10.1016/J.JHYDROL.2016.02.041

[46] Bohling, G.C. Liu, G., Dietrich, P., Butler, J.J.Jr., 2016. Reassessing the MADE direct-push hydraulic conductivity data using a revised calibration procedure. Water Resources Research, 52(11):8970-8985, 10.1002/2016WR019008

[47] Dougherty, D.E., Babu, D.K., 1984. Flow to a partially penetrating well in a double-porosity reservoir, Water Resour. Res. 20 (8): 1116–1122, 10.1029/WR020i008p01116

[48] Vasco, D.W., Datta-Gupta, A., Long, J.C.S., 1997. Resolution and uncertainty in hydrologic characterization. Water Resour. Res., 33(3), 379-397, 10.1029/96WR03301

[49] Hansen, P.C., 2023. Regularization tools: A MATLAB package for analysis and solution of discrete ill-posed problems. Version 4.1. regtools

(https://www.mathworks.com/matlabcentral/fileexchange/52-regtools), MATLAB Central File Exchange. Retrieved February 6, 2023.

[50] Moore, E.H., 1920. On the reciprocal of the general algebraic matrix. Bulletin of the American Mathematical Society, 26, 394-395.

[51] Penrose, R., 1955. A generalized inverse for matrices. Proc. Cambridge. Philos. Soc., 51, 406-413.

[52] Tikhonov, A.N., Goncharsky, A.V., 1987. Ill–Posed Problems in the Natural Sciences. MIR Publishers, Moscow.

[53] Hansen, P.C., 1992. Analysis of discrete ill-posed problems by means of the L-curve. SIAM Review, 34(4): 561-580.

[54] Hansen, P.C., Toke, J., Giuseppe, R., 2007. An adaptive pruning algorithm for the discrete L-curve criterion. Journal of Computational and Applied Mathematics, 198: 483-492, 10.1016/j.cam.2005.09.026

[55] Günther, T., 2004. Inversion Methods and Resolution Analysis for the 2D/3D Reconstruction of Resistivity Structures from DC Measurements. Ph.D. Thesis, Technische Universität Bergakademie Freiberg, 160 pp.

[56] Jacob, C.E., 1950. Flow of groundwater, in Engineering Hydraulics, edited by H. Rouse, John Wiley, New York, p321-386.

[57] Copty, N.K., Findikakis, A.N., 2004. Stochastic analysis of pumping test drawdown data in heterogeneous geologic formations, Journal of Hydraulic Research, 42:S1, 59-67, DOI: 10.1080/00221680409500048

[58] Cheng, Y., Renner, J., 2021. Constraints on hydraulic anisotropy from periodic pumping tests using a double-packer system. Water Resources Research, 57, e2020WR027753, 10.1029/2020WR027753

Author statement

Daniel Paradis: Conceptualization, Methodology, Software, Formal analysis, Validation, Writing- Original draft **René Lefebvre**: Conceptualization, Methodology, Writing- Review and Edit **Aymen Nefzi**: Writing- Reviewing and Editing

Declaration of interests

☐ The authors declare that they have no known competing financial interests or personal relationships that could have appeared to influence the work reported in this paper.

☒ The authors declare the following financial interests/personal relationships which may be considered as potential competing interests:

Paradis reports financial support was provided by Geological Survey of Canada (Quebec). Paradis reports a relationship with Geological Survey of Canada (Quebec) that includes: employment.